Critical phenomena and quantum phase transition in long range Heisenberg antiferromagnetic chains

Nicolas Laflorencie, Ian Affleck and Mona Berciu

Department of Physics and Astronomy, University of British Columbia, Vancouver, BC, V6T 1Z1, Canada
E-mail: laflo@physics.ubc.ca, iaffleck@physics.ubc.ca and berciu@physics.ubc.ca

Abstract. Antiferromagnetic Hamiltonians with short range, non-frustrating interactions are well known to exhibit long range magnetic order in dimensions $d \geq 2$ but exhibit only quasi-long-range order, with power-law decay of correlations, in $d = 1$ (for half-integer spin). On the other hand, non-frustrating long range interactions can induce long range order in $d = 1$. We study Hamiltonians in which the long range interactions have an adjustable amplitude λ, as well as an adjustable power law $1/|x|^{\alpha}$, using a combination of quantum Monte Carlo and analytic methods: spin-wave, large N non-linear σ model, and renormalization group methods. We map out the phase diagram in the λ–α plane and study the nature of the critical line separating the phases with long range and quasi-long-range order. We find that this corresponds to a novel line of critical points with continuously varying critical exponents and a dynamical exponent, $z < 1$.

Contents

1. Introduction

The ground state (GS) of the nearest neighbour antiferromagnetic (AF) Heisenberg model on a bipartite lattice,

$$\mathcal{H} = \sum_{\langle i,j \rangle} \vec{S}_i \cdot \vec{S}_j, \tag{1}$$

is generally expected to have long range order (LRO):

$$\langle \vec{S}_0 \cdot \vec{S}_r \rangle \to \pm m_{\mathrm{AF}}^2, \qquad (r \to \infty), \tag{2}$$

for any spin magnitude, S and any dimension $d \geq 2$ [1]. On the other hand, in dimension $d = 1$, the behaviour depends on whether S is integer or half-integer [2]. In the half-integer case the spin–spin correlation function

$$\langle \vec{S}_0 \cdot \vec{S}_r \rangle \propto \frac{(-1)^r \sqrt{\ln r}}{r}, \tag{3}$$

is expected [3], characteristic of a *quasi*-long range order (QLRO). (In the integer spin, Haldane gap case, correlations decay exponentially.) This behaviour in $d = 1$ for half-integer S is believed to be universal, not depending on the magnitude of S or on the details of the Hamiltonian as long as it is short range and not too frustrating. Long range interactions (i.e. power law decaying with the relative distance between interacting moments) can be introduced in spin models either for some experimental reasons like dipolar or RKKY interactions or simply because of some theoretical relevance. For instance, a famous example is the Haldane–Shastry model [4] with AF frustrating $1/r^2$ interaction which exhibits an exact RVB GS. Another theoretical interest comes from the possibility to interpolate between discrete dimensions by tuning continuously the exponent that governs the decay of the interaction with the distance. Indeed, the possibility for true LRO to occur in $d = 1$ with long range interactions has motivated many studies during the last decades [5]–[14] and is the subject of the present paper. While a long standing debate about the critical behaviour of the Ising model in d dimensions with long range ferromagnetic interaction decaying like $r^{-d-\sigma}$ has been quite intense during the last 30 years [6, 11, 12], the N-vector model has also been a subject of interest for many authors [7]–[10]. Concerning the Heisenberg model with long range interaction $\sim r^{-\alpha}$, the seminal paper of Mermin and Wagner [5] proving the absence of LRO at finite temperature T in $d \leq 2$ for $\alpha > d + 2$ has been recently reconsidered by Bruno [13], who gave stronger conditions for the absence of spontaneous magnetic order at $T > 0$ in $d \leq 2$. For instance, he proved that the AF non-frustrating one-dimensional model

$$\mathcal{H} = \sum_i \left[\vec{S}_i \cdot \vec{S}_{i+1} - \lambda \sum_{j=2}^{\infty} (-1)^j \frac{\vec{S}_i \cdot \vec{S}_{i+j}}{j^\alpha} \right] \tag{4}$$

does not have Néel order for any temperature $T > 0$ if $\alpha \geq 2$. Actually, much less is known about the $T = 0$ case, except the work of Parreira *et al* [15], where the authors signalled the existence of the bound $\alpha = 3$ over which $T = 0$ LRO is ruled out[1]. A

---

[1] The proof for non-existence of LRO at $T = 0$ for $\lambda = 1$, if $\alpha > 3$ [15], can be trivially extended and shown to hold for all $\lambda \neq 1$.

particular case, the model (4) with $\lambda = 1$, was recently analysed at both $T = 0$ and $T > 0$ in [14], using the lowest order spin-wave (SW) approximation, expected to be valid for large enough S and small enough α. There it was shown that the SW dispersion relation takes the *sublinear* form, at low k:

$$\omega(k) \propto |k|^{(\alpha-1)/2}, \tag{5}$$

for $\alpha < 3$. Consequently the quantum $1/S$ reduction of the order parameter,

$$\Delta m_q \propto \int \frac{\mathrm{d}k}{\omega(k)}, \tag{6}$$

is finite for any $\alpha < 3$. By requiring that $\Delta m_q < S$, a consistency condition on the SW approximation, it is concluded that LRO occurs for any S at sufficiently small α. (However, such an estimate is presumably only reliable for $S \gg 1$.) After correcting a numerical error in [14], the SW prediction for the $S = 1/2$, $\lambda = 1$ case is existence of Néel order at $T = 0$ for $\alpha < \alpha_c^{\mathrm{sw}} = 2.46$.

In this work, we extend the results of Yusuf *et al* in several ways, focusing on the zero-temperature behaviour of the non-frustrating spin $1/2$ Hamiltonian (4) with long range interaction of adjustable strength λ and exponent α. In section 2, we consider the relevance of the long range term as a perturbation to the nearest neighbour interaction, using a simple heuristic argument of mean-field type as well as the power-counting of the scaling dimension of the perturbation. For $\lambda \ll 1$, we find that the long range perturbation is marginal if $\alpha = 2$ and relevant (irrelevant) for $\alpha < 2$ ($\alpha > 2$). We then investigate the α- and λ-dependence of the critical behaviour using various techniques. We begin, in section 3, with semi-classical calculations: the SW expansion and a large N approximation based on the non-linear σ model. Both approximations give qualitatively similar phase boundaries, and sublinear dispersion like in equation (5) in the ordered phase. Some of the critical exponents can also be estimated within these approximations. However, the results obtained in the SW or large N approximations are not quantitatively correct. We therefore use large scale numerical simulations to investigate more precisely the phase diagram of this model in sections 4 and 5. We study systems of up to $L = 4000$ sites using quantum Monte Carlo (QMC) methods, based on a stochastic series expansion (SSE) of the partition function [16, 17]. We verify that for $S = 1/2$ there are indeed stable phases with both QLRO given by equation (3) and with true Néel LRO (equation (2)). We accurately determine the phase boundary, as well as some of the critical exponents which are found to vary continuously along the critical line. In section 6, we also apply analytic renormalization group (RG) methods to investigate the case $\lambda \ll 1$. Section 7 contains conclusions. In two appendices we gives further details on the spin-wave theory and large N calculations.

2. Relevance of the perturbation: mean field and scaling arguments

Let us consider a short range spin $1/2$ chain with an additional long range perturbation of the form

$$\sum_{r,r'} J(r,r') \vec{S}_r \cdot \vec{S}_{r'}, \tag{7}$$

with

$$J(r, r') = -\frac{(-1)^{|r-r'|}}{|r - r'|^\alpha}. \tag{8}$$

Following an argument given by Cardy [18] for the relevance of a long range perturbation, we can in first approximation look at the mean field correction to the free energy coming from this long range term (7):

$$\delta F = \sum_{r,r'} J(r, r') \langle \vec{S}_r \cdot \vec{S}_{r'} \rangle, \tag{9}$$

where $\langle \cdots \rangle$ is evaluated in the unperturbed system where we know the behaviour of the correlation function

$$\langle \vec{S}_r \cdot \vec{S}_{r'} \rangle \sim \frac{(-1)^{|r-r'|}}{|r - r'|^{z+\eta-1}}. \tag{10}$$

In a finite system of length L, the change in the free energy per site δf thus scales like

$$\delta f \sim \int_1^L \frac{\mathrm{d}r}{r^{\alpha+z+\eta-1}}. \tag{11}$$

The integral above will give a constant term and a size dependent term

$$\delta f(L) \sim L^{2-\alpha-z-\eta} \sim L^{-\alpha}, \tag{12}$$

where we have used the fact that $z = \eta = 1$ in the short range QLRO regime of the spin $1/2$ chain. Then, we can compare this with the usual finite size corrections to the free energy of the conformally invariant short range $S = 1/2$ chain which are known to scale like L^{-2} to lowest order [19]. This tells us that (to first order perturbation) if $\alpha < 2$ the long range perturbation creates a correction which dominates the L^{-2} correction of the unperturbed fixed point and is probably a relevant perturbation for the short range model.

Another way of deriving this result is to compute the scaling dimension of the perturbation, based on the usual continuum formulation of the short range model in which uniform and staggered magnetization density operators, $(\vec{J}_{\mathrm{L}} + \vec{J}_{\mathrm{R}})$ and $\vec{n}$, are introduced:

$$\vec{S}(x) \approx (\vec{J}_{\mathrm{L}} + \vec{J}_{\mathrm{R}}) + (-1)^x \vec{n}(x). \tag{13}$$

Only slowly varying Fourier modes of the fields $\vec{J}_{\mathrm{L/R}}(x)$ and $\vec{n}(x)$ are present in the low energy effective Hamiltonian. $\vec{J}_{\mathrm{L/R}}$ are the conserved left/right-moving spin densities. Ignoring a marginally irrelevant interaction, the staggered magnetization field, $\vec{n}$, has the Green's function

$$\langle n^a(z) n^b(0) \rangle = \frac{\delta^{ab}}{|z|}, \tag{14}$$

with $z \equiv \tau + \mathrm{i}x$. The long range perturbation adds to the low energy, continuum limit of the imaginary time action, a term of the form

$$\delta S[\vec{n}] \sim -\lambda \int \frac{\mathrm{d}\tau \, \mathrm{d}x \, \mathrm{d}y}{|x - y|^\alpha} \vec{n}(\tau, x) \cdot \vec{n}(\tau, y). \tag{15}$$

Utilizing the fact that, from equation (14), $\vec{n}$ has a scaling dimension of $1/2$, a simple power counting tells us that the perturbation is irrelevant for $\alpha > 2$, relevant for $\alpha < 2$, and marginal for $\alpha = 2$. Also note that $\lambda > 0$ corresponds to non-frustrating interactions which favour the Néel state with $\langle n^z \rangle \neq 0$.

3. Spin-wave expansion and large N approximation

3.1. Spin-wave expansion

This calculation simply generalizes that of Yusuf *et al* in [14], to $\lambda \neq 1$. We summarize here the main steps. Some further results are given in appendix A. On the LRO side of the transition, we use the Holstein–Primakoff approximation [20]:

$$S_i^z = S - a_i^\dagger a_i, \qquad S_i^+ \approx \sqrt{2S} a_i, \qquad S_i^- \approx \sqrt{2S} a_i^\dagger,$$

for i odd and

$$S_j^z = b_j^\dagger b_j - S, \qquad S_j^+ \approx \sqrt{2S} b_j^\dagger, \qquad S_j^- \approx \sqrt{2S} b_j,$$

for j even, and retain only the quadratic terms in the Hamiltonian (4). After a Fourier transform over the reduced Brillouin zone $k \in (-\pi/2a, \pi/2a)$, we find

$$\mathcal{H}_{\mathrm{SW}} \approx S \sum_k \left[(\gamma - f(k)) \left(a_k^\dagger a_k + b_k^\dagger b_k \right) + g(k) \left(a_k^\dagger b_{-k}^\dagger + b_{-k} a_k \right) \right] + \cdots \tag{16}$$

where, for an infinite chain[2],

$$\gamma = 2 + 2\lambda \sum_{n=2}^{\infty} \frac{1}{(2n-1)^\alpha}$$

$$f(k) = 2\lambda \sum_{n=1}^{\infty} \frac{\cos(2kna) - 1}{(2n)^\alpha}$$

$$g(k) = 2\cos(ka) + 2\lambda \sum_{n=2}^{\infty} \frac{\cos[k(2n-1)a]}{(2n-1)^\alpha}.$$

This quadratic Hamiltonian can be diagonalized with a Bogoliubov transformation to

$$\mathcal{H}_{\mathrm{SW}} \approx S \sum_k \omega_k \left(\chi_{k,1}^\dagger \chi_{k,1} + \chi_{k,2}^\dagger \chi_{k,2} \right) \tag{17}$$

with an SW spectrum

$$\omega_k = \sqrt{[\gamma - f(k)]^2 + [g(k)]^2} \xrightarrow{k \to 0} k^{(\alpha-1)/2}, \tag{18}$$

as discussed above. At $T = 0$, the correction to the staggered magnetization at any site is

$$\Delta m_q = \langle a_i^\dagger a_i \rangle = \langle b_j^\dagger b_j \rangle = \frac{a}{2\pi} \int_{-\pi/2a}^{\pi/2a} \mathrm{d}k \left[\frac{\gamma - f(k)}{\omega_k} - 1 \right].$$

The consistency condition $\Delta m_q < S$ then allows us to find the SW approximation for the value of α_c^{sw} below which long range Néel order is established. As already stated, for $S = 1/2$ and $\lambda = 1$, we find $\alpha_c^{\mathrm{sw}} = 2.46$. A plot of α_c^{sw} versus λ, for $S = 1/2$, is shown in figure 1.

---

[2] These equations are the analogues of equations (6) of [14]. We use γ instead of α since in our work α defines the spatial variation of the exchange (the parameter called β in [14]). The definition of $f(k)$ is corrected by a factor of 2.
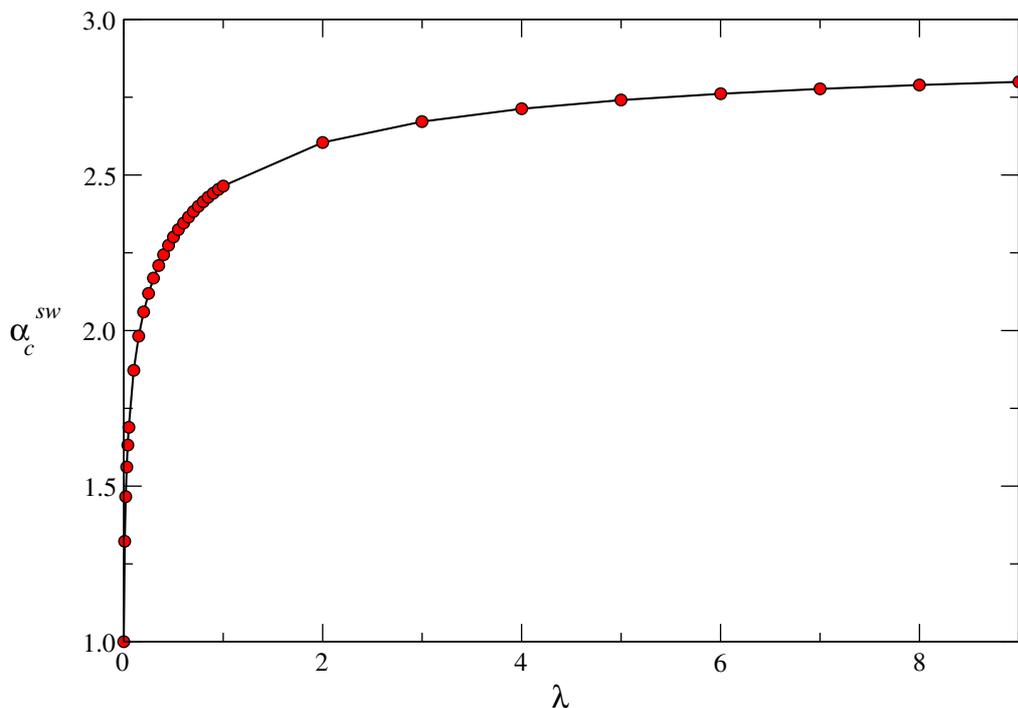
Figure 1. Spin-wave approximation prediction for the value $\alpha_{\rm c}^{\rm sw}$ below which long range Néel order is expected at $T = 0$, as a function of λ and for $S = 1/2$. The critical curve saturates at $\alpha \simeq 2.9032$ when $\lambda \to \infty$.

This phase boundary given by the lowest order SW approximation turns out not to be quantitatively correct, as we are going to see with the QMC results presented in section 4. In particular, it happens that SW predictions miss the fact that the critical line goes to $\alpha = 2$ when $\lambda \to 0$. Nevertheless SW predictions are, to some extent, shared by large N calculations as we are going to see below.

3.2. Large N approximation

The details of this calculation are given in appendix B. Here we present the main steps and discuss the results which come from this approximation. We generalize the Néel order parameter field, $\vec{n}(\tau, x)$ appearing in equation (13), to an N-component field and take the limit of large N. In this approximation two phases occur in the λ–α plane. The critical line terminates at $\alpha = 1$, as in the spin-wave approximation. These two phases are a phase with Néel order and a disordered phase with a finite correlation length. (The unusual quasi-long-range ordered phase is special to the case $N = 3$ and is not captured by the large N approximation.) Along the critical line separating these two phases the mean field result, $\eta = 3 - \alpha$, is obtained. The dynamical exponent takes the value $z = (\alpha - 1)/2$, corresponding to the dispersion relation $\omega \propto |k|^{(\alpha-1)/2}$ also obtained in spin-wave theory. The correlation length diverges with an exponent ν defined by

$$\xi \propto |\lambda_{\rm c} - \lambda|^{-\nu}, \tag{19}$$

with

$$\nu = \begin{cases} 1/(\alpha - 1), & (1 < \alpha < 5/3) \\ 2/(3 - \alpha), & (5/3 < \alpha < 3). \end{cases} \tag{20}$$

4. Quantum Monte Carlo results I: finite size effects

In this section, we present results obtained using the QMC SSE method based on directed loop updates [16]. This algorithm, used here to investigate the model (4), has been proposed recently by Sandvik [17] to study spin Hamiltonians with non-frustrating long range interactions.

4.1. Finite size corrections

We first focus on the $\lambda = 1$ case, studied by SW in [14], governed by the following Hamiltonian:

$$\mathcal{H} = -\sum_{i,j \geq 1} \frac{(-1)^j}{j^\alpha} \vec{S}_i \cdot \vec{S}_{i+j}. \tag{21}$$

In order to detect a Néel instability at the thermodynamic limit, we compute the staggered structure factor, normalized per site, on finite length spin $S = 1/2$ chains, defined by

$$S_\pi(L) = \frac{1}{L^2} \sum_{i,j} (-1)^{i-j} \langle \vec{S}_i \cdot \vec{S}_j \rangle = \frac{3}{L^2} \left\langle \left(\sum_{i=1}^{L} (-1)^i S_i^z \right)^2 \right\rangle. \tag{22}$$

We have performed SSE simulations for different system sizes, up to $L_{\max} = 4096$, at temperatures $\beta^{-1} = 1/2L$ low enough to get the GS properties. Results for $S_\pi(L)$ are shown versus $1/L$ in the left panel of figure 2 for different values of the power-law exponent α. The staggered structure factor displays two types of behaviour: for small values of α it saturates to a finite non-zero number, whereas for large enough α, $S_\pi(L)$ vanishes when $L \to \infty$. Then, in order to extract the thermodynamic limit behaviour of S_π, we perform a finite size analysis in order to get the AF order parameter, given by

$$\sqrt{S_\pi(L)} \to m_{\text{AF}}, \qquad (L \to \infty). \tag{23}$$

Utilizing the fact that in the QLRO regime the spin–spin correlation functions decay as stated in equation (3), we therefore expect in this regime the following behaviour for the staggered structure factor per site:

$$S_\pi(L) = \frac{1}{L} \int_1^L (-1)^r \langle \vec{S}_0 \cdot \vec{S}_r \rangle \mathrm{d}r \sim \frac{(\ln L)^{3/2}}{L}, \qquad (L \to \infty). \tag{24}$$

On the other hand, in the Néel phase, the finite size scaling of the order parameter can be evaluated using the small k SW spectrum (see appendix A), leading to

$$S_\pi(L) - m_{\text{AF}}^2 \sim L^{(\alpha-3)/2} + \mathrm{O}(L^{\alpha-3}). \tag{25}$$

We used second order polynomial fits in $L^{(\alpha-3)/2}$ to extrapolate the finite size data to their thermodynamic limit values, shown in the right panel of figure 2. The quantum phase
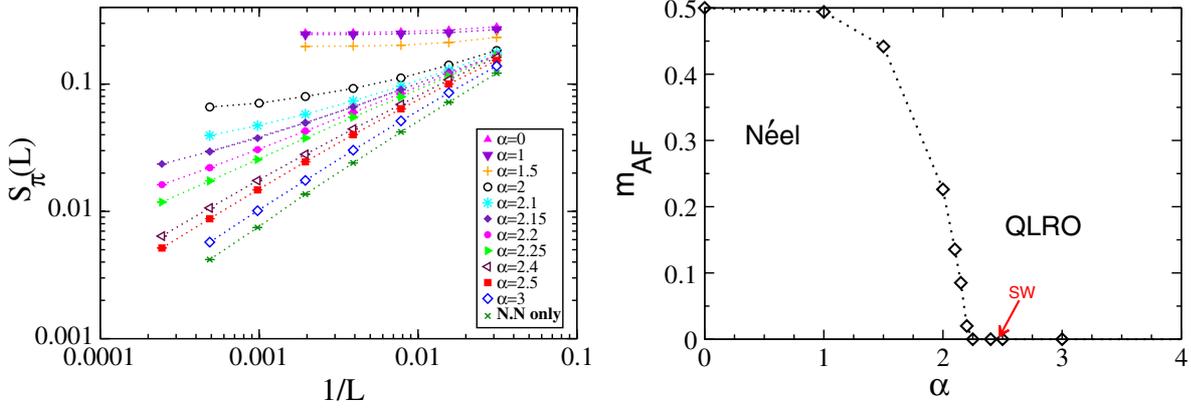
Figure 2. Left panel: $T = 0$ QMC results for the staggered structure factor per site $S_\pi(L)$ computed in the GS for the Hamiltonian (21) and plotted versus the inverse system size L^{-1} in a log–log scale. Different symbols are used for different values of the power-law exponent α, as indicated on the plot. The case with only nearest neighbour interactions is also shown (N.N green crosses) for comparison. Right panel: infinite size AF order parameter m_{AF} plotted versus α, obtained using finite size scaling of $S_\pi(L)$ (shown on the left panel). The quantum phase transition between the Néel phase ($m_{AF} \neq 0$) and the QLRO phase ($m_{AF} = 0$) occurs at $\alpha_c = 2.225 \pm 0.025$. The SW estimate ($\alpha_c^{sw} \simeq 2.46$) is indicated by the arrow.

transition between the AF Néel order and the QLRO phase is clearly visible for a critical value $2.2 < \alpha_c < 2.25$. It is also interesting to compare this estimate with the one from the SW approximation giving $\alpha_c^{sw} \simeq 2.46$.

Let us now concentrate on the α- and λ-dependent Hamiltonian (4) by keeping a fixed value for α while varying λ. We first focus on the case with $\alpha = 2.1$, which is expected to display a transition for a non-zero value of λ. As pointed out by Reger and Young, studying finite size AF clusters in $d = 2$ [21], the sublattice (infinite size) magnetization can be obtained either from the staggered structure factor (equation (23)) or from the correlation functions at the largest separation

$$C(L) = \langle \vec{S}_i \cdot \vec{S}_{i+L/2} \rangle \rightarrow \pm m_{AF}^2, \qquad (L \rightarrow \infty). \qquad (26)$$

In the Néel phase, both estimators $S_\pi(L)$ and $C(L)$ are expected to converge to m_{AF}^2 with a similar power-law behaviour but with different pre-factors. This feature is illustrated by the computation of $C(L)$ and $S_\pi(L)$ for $\alpha = 2.1$ and four different values of the long range term strength $\lambda = 3, 2, 0.9$ and 0.6, as shown in figure 3. Using second order polynomial fits in $L^{(\alpha-3)/2}$, we can obtain infinite size extrapolated values for $m_{AF}(\lambda)$ from $S_\pi(L)$ or $C(L)$, as reported in table 1. Finite size effects are more pronounced for the staggered structure factor than for the mid-chain correlation function because $S_\pi(L)$ is the result of the integration of the staggered correlation function along the entire chain and therefore is sensitive to short distance terms. However, the estimates for the sublattice magnetization obtained from $C(L)$ and $S_\pi(L)$ (see table 1) are both in good agreement, especially when the system is deeply in the Néel regime (large values of λ). On the other hand, when the system is approaching the quantum critical point (QCP) where $m_{AF} \rightarrow 0$, the finite size
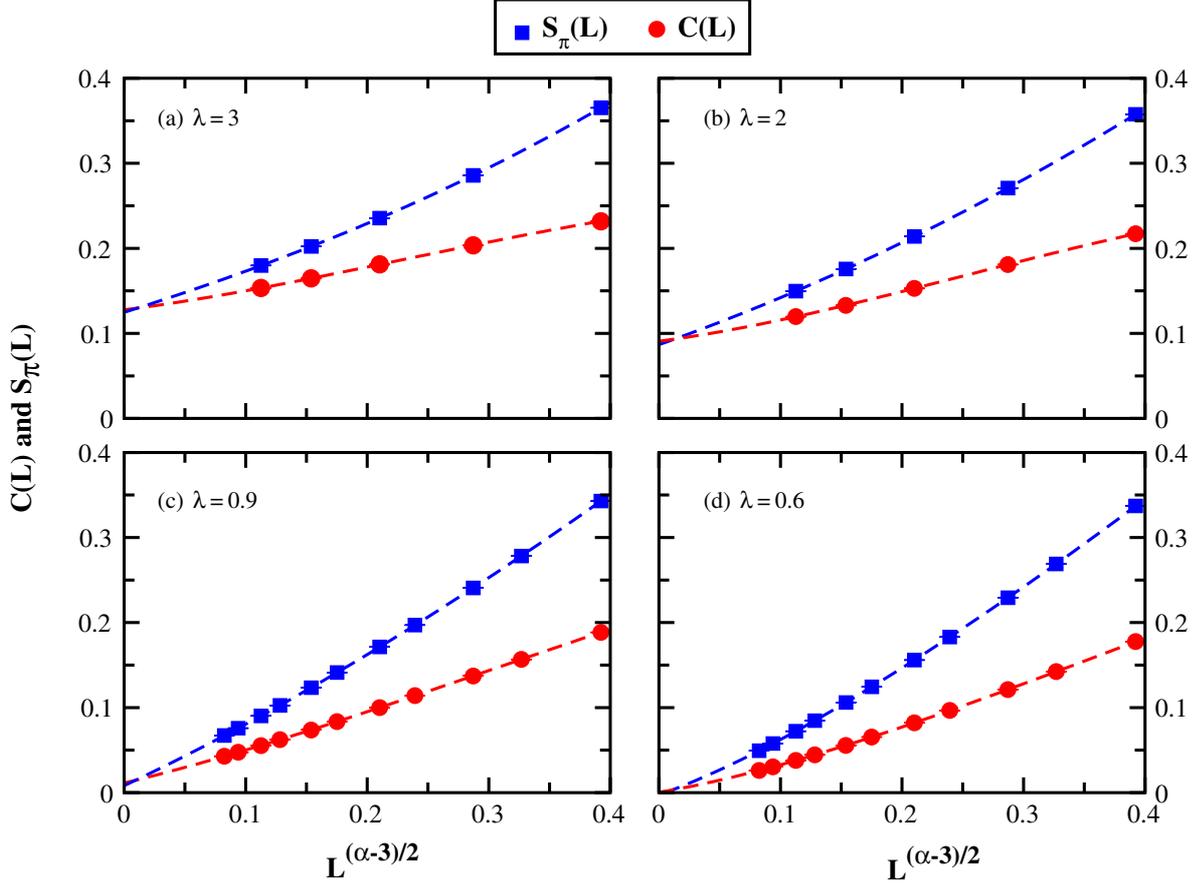
Figure 3. Staggered structure factor per site $S_\pi(L)$ (equation (23)) and mid-chain correlation function $C(L)$ (equation (26)) computed at $T = 0$ with QMC for $\alpha = 2.1$ and four different values of λ, as shown in plots (a)–(d). Finite size scaling has been performed on finite systems up to $L_{\max} = 128$ for the largest values of λ ((a) and (b)) and up to $L_{\max} = 256$ for the smallest ((c) and (d)). The dashed lines are polynomial fits of the form $m_{\mathrm{AF}}^2 + a_1 L^{(\alpha-3)/2} + a_2 L^{\alpha-3}$.

Table 1. Infinite size extrapolated values of the sublattice magnetization m_{AF} obtained for $\alpha = 2.1$ and $\lambda = 3$, 2, 0.9, and 0.6 from power-law fits of the staggered structure factor $S_\pi(L)$ and the mid-chain correlation function $C(L)$ (see figure 3).

λ	m_{AF} from $S_\pi(L)$	m_{AF} from $C(L)$
3	0.353	0.356
2	0.295	0.301
0.9	0.106	0.091
0.6	0	0.02

effects are significant enough to prevent us from obtaining a very precise estimate of the critical coupling λ_c where the AF LRO vanishes.

Of course, in principle it is possible to perform very large scale numerical SSE simulations on the largest reachable system sizes, as we did for the $\lambda = 1$ case with
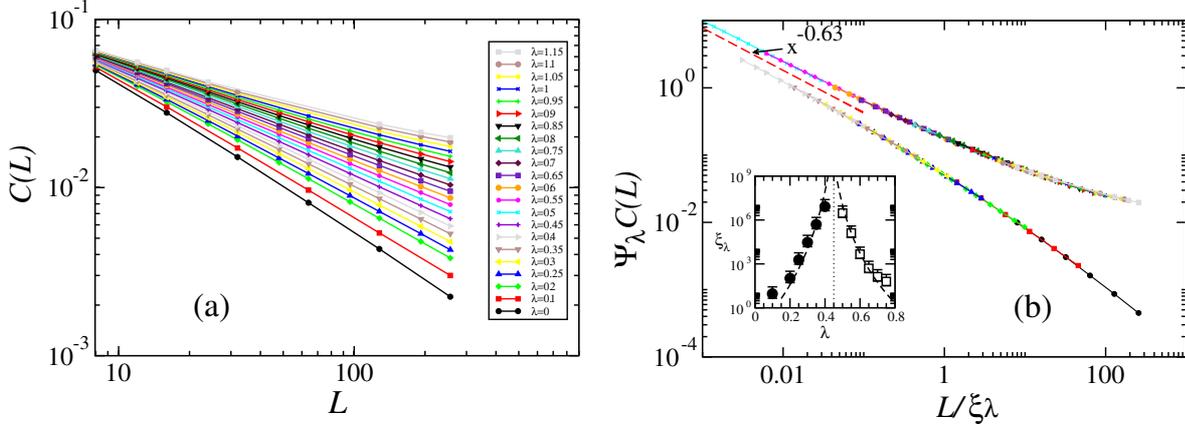
Figure 4. $T = 0$ QMC results for the mid-chain correlation function $C(L)$ computed for $\alpha = 2.1$ and different values of λ, as indicated on the plot. (a) $C(L)$ is plotted versus the system size L for $0 \le \lambda \le 1.15$. (b) Both x- and y-axis are rescaled using two parameters: the crossover length scale ξ_λ and Ψ_λ. The data collapse results in two universal curves: one for the Néel ordered phase (top one) and one for the QLRO regime (lower one). Note that for clarity the QLRO universal curve has been shifted downwards. The red dashed line materializes the critical separatrix between the two regimes, decaying with an exponent $\simeq 0.63$. Inset: crossover length scale ξ_λ extracted from the data collapse in the QLRO (full circles) and Néel regimes (open squares). The dashed lines are power-law fits of the form $|\lambda - \lambda_c|^{-\nu}$ with $\lambda_c \simeq 0.45$ (indicated by vertical dotted line) and $\nu \sim 15$.

$L_{\max} = 4096$. However, since our goal here is to investigate the quantum critical phenomena in the λ–α plane, we need a good sampling of this parameter space and we therefore restrict the simulations over systems of maximum size $L_{\max} \le 1024$. We then use another strategy, based on scaling arguments, to perform a better data analysis close to criticality. This is described next.

4.2. Scaling analysis

As previously discussed, the finite size effects are bigger for the staggered structure factor than for the mid-chain correlation function. Therefore, we now focus on $C(L)$, which is expected to saturate to a constant value in the Néel phase, whereas in the QLRO regime the behaviour $C(L) \to \sqrt{\ln(L/a)}/L$ is expected, a being a non-universal constant.

In order to illustrate the scaling analysis, let us continue to study the case with $\alpha = 2.1$, as in the previous subsection. We have computed $C(L)$ for several values of the long range coupling strength λ in the range $[0, 1.15]$, for sizes up to $L = 256$. The results, shown in figure 4(a), clearly show the existence of a finite critical value λ_c which separates the QLRO and the Néel regimes. In order to locate precisely this QCP, let us assume that a typical length scale ξ_λ governs a crossover from the QCP to the Néel phase if $\lambda > \lambda_c$ and from the QCP to the QLRO regime if $\lambda < \lambda_c$. Precisely at the critical point, the spin–spin correlation function decays like a power law

$$C_{\text{QCP}}(L) \sim L^{1-z-\eta}, \tag{27}$$

thus defining the critical exponents η and z, the critical dynamical exponent. Without making any assumption about the values of the aforementioned critical exponents, let us now define scaling functions $f_{\pm}(x)$, with $x = L/\xi_{\lambda}$, for $\lambda > \lambda_{\rm c}$ and $\lambda < \lambda_{\rm c}$, respectively, by

$$f_{\pm}(x) = \frac{C(L)}{C_{\rm QCP}(L)}. \tag{28}$$

Hence, the scaling functions obey

$$\begin{aligned}
f_{-}(x) &\propto x^{-2+z+\eta}\sqrt{\ln x} && \text{if } x \gg 1 \quad \text{and} \quad \lambda < \lambda_{\rm c} \quad \text{(QLRO)} \\
f_{+}(x) &\propto x^{-1+z+\eta} && \text{if } x \gg 1 \quad \text{and} \quad \lambda > \lambda_{\rm c} \quad \text{(NEEL)} \\
f_{\pm}(0) &= 1 && \text{if } \lambda \simeq \lambda_{\rm c} \quad \text{(QCP)}.
\end{aligned} \tag{29}$$

It is convenient to also rescale the y-axis with the unknown function Ψ_{λ} in order to get $C(L) \times \Psi_{\lambda} = f(x) \times x^{1-z-\eta}$. We then expect Ψ_{λ} to be proportional to $\xi_{\lambda}^{z+\eta-1}$. Using such scaling forms, we have obtained the collapse of the data shown in figure 4(a) into two universal curves shown in figure 4(b). The parameters ξ_{λ} and Ψ_{λ} have been chosen to give the best data collapses. Using such a scaling analysis, we find a critical coupling $\lambda_{\rm c} = 0.45 \pm 0.05$ that we can compare to the overestimated value $\lambda_{\rm c} = 0.6$ previously found using the simpler finite size scaling equation (25). The critical correlation (given by the separatrix between the two regimes in figure 4(b)) is characterized here by a power-law decay with an exponent $(z + \eta - 1)_{\rm QCP} \simeq 0.63$. Note also that the crossover length scale ξ_{λ}, plotted in the inset of figure 4(b), diverges on both sides of the transition with a large exponent $\nu \sim 15$.[3] These and other issues related to the critical exponents will be discussed in detail in section 5.3.

5. Quantum Monte Carlo II: phase diagram and critical behaviour

The scaling analysis described above has been repeated for several values of α in order to explore and construct the phase diagram of the model (4) in the λ–α plane.

5.1. $\alpha = 2$: marginal case

Let us first focus on the marginal case with $\alpha = 2$, for which a similar data collapse analysis is performed and shown in figure 5 for the mid-chain correlation function.

Using QMC simulations results for chains up to $L = 512$ sites, with $\lambda \in [0, 3]$, we have been able to get a universal curve (see figure 5) which shows a crossover towards a Néel order phase (i.e. $C(L) \to$ constant if $L \gg \xi_{\lambda}$). Note that for $\lambda < 0.1$ the typical length scale necessary to get a good collapse becomes very large so that there is no overlap between our different curves and the data collapse analysis is impossible to achieve. Nevertheless, the crossover length scale ξ_{λ}, plotted in the inset of figure 5, displays an exponential divergence when $\lambda \to 0$. Guided by the RG calculations presented

---

[3] A precise determination of the exponent ν is actually impossible to achieve because of large error bars for ξ_{λ} due to some natural uncertainties in the data collapse procedure.
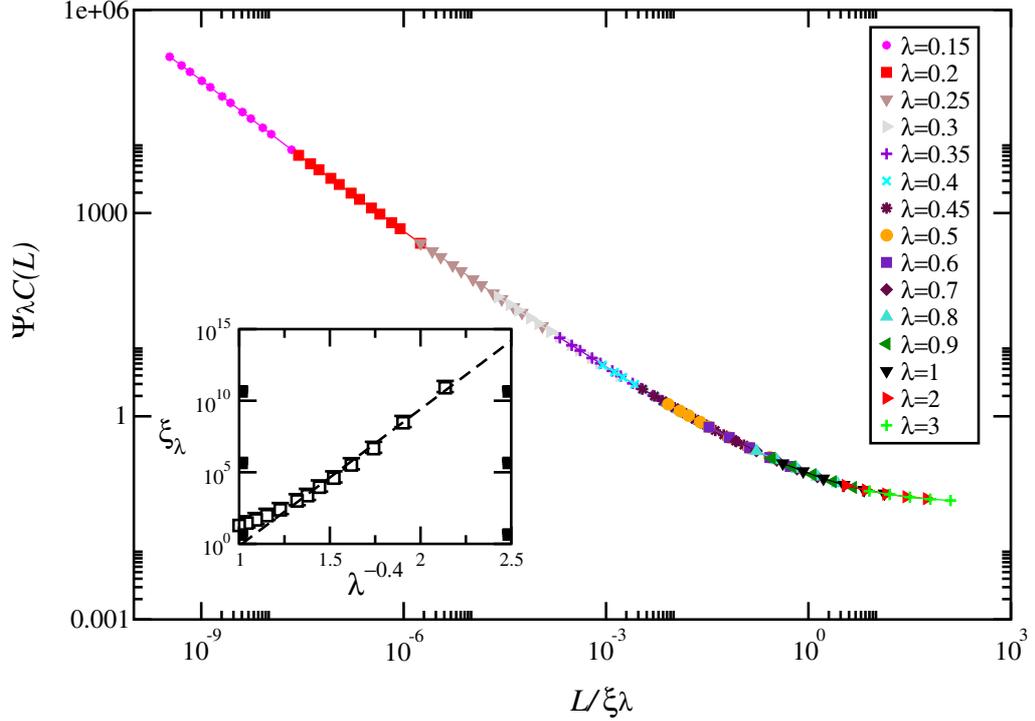
Figure 5. $T = 0$ QMC results at $\alpha = 2$ for the mid-chain correlation functions $C(L)$. As in figure 4, both x- and y-axes have been rescaled in order to get the best data collapse. For the different values of λ indicated on the plot, the data collapse on a unique crossover curve towards the Néel ordered phase. Inset: crossover length scale ξ_λ plotted in a linear–log scale versus $\lambda^{-0.4}$. The dashed line is a fit of the form equation (30) with $\sigma = 0.4$.

in section 6, we can fit the λ-dependence of the crossover length scale by

$$\xi_\lambda \sim \exp(C/\lambda^\sigma), \tag{30}$$

with $\sigma = 0.4$ and C being a free parameter. It is however important to note that since ξ_λ suffers from large error bars, and so does the fitting parameter, we have forced σ to its value found in equation (66).

Unambiguously, ξ_λ is found to diverge when $\lambda \to 0$, which means that at the marginal point $\alpha = 2$ any $\lambda > 0$ will drive the system towards the Néel phase. In other words, the long range interaction perturbation of strength λ is *marginally relevant* at $\alpha = 2$. This result agrees with the RG calculations presented in section 6.

5.2. Phase diagram

As previously stated, when $\alpha \leq 2$ the long range interaction is a relevant perturbation and any $\lambda > 0$ will drive the QLRO phase towards a AF ordered Néel phase with $m_{\mathrm{AF}} \neq 0$. On the other hand, when $\alpha > 2$ a simple power-counting tells us that the perturbation is irrelevant, which should imply that the QLRO is stable against a small perturbation $\lambda > 0$. It turns out that such a simple argument is not sufficient to provide a correct description of the quantum critical behaviour of the system (see the next section for a
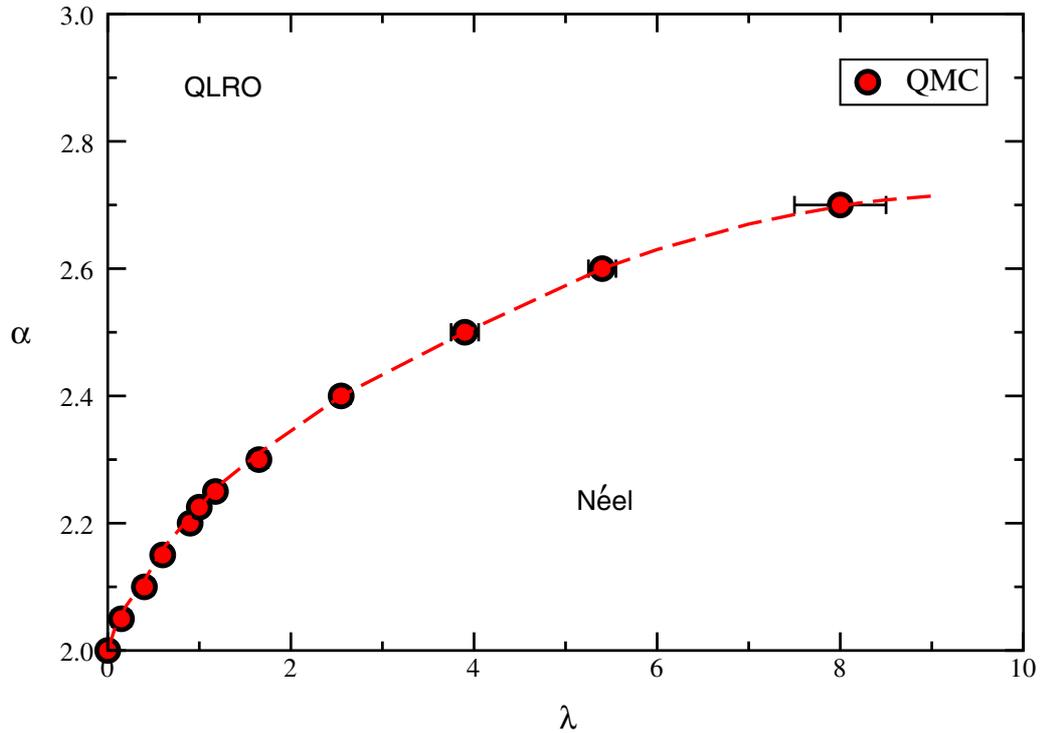
Figure 6. $T = 0$ phase diagram of the long range $S = 1/2$ model (equation (4)) computed by large scale QMC simulations and plotted in the λ–α plane. A line of critical points (circles) separates a long range ordered phase (Néel) and a quasi-long-range ordered phase (QLRO). The error bars, due to some uncertainties in the finite size scaling analysis of the numerical data, are explicitly show on the plot. The dashed line is a guide for the eyes.

more advanced field theoretical description). Based on large scale numerical simulations, we provide hereafter a picture which is consistent with the existence of a non-trivial line of fixed points in the λ–α plane.

Using QMC simulations on systems of up to $L = 1000$, we performed the scaling analysis for the mid-chain correlation function $C(L)$ as well as for the staggered susceptibility (see below) and computed the phase diagram for $2 \leq \alpha \leq 2.7$. For each value of α, the QCP λ_c is found by the separatrix between the two crossover functions (see figure 4(b)) with some error bars due to the discrete sampling in the λ space as well as the strong divergence of the crossover length scale close to the critical point which makes the data collapse delicate. We present in figure 6 the QMC phase diagram in the λ–α plane. As discussed, λ is marginally relevant at $\alpha = 2$, driving the system towards a Néel phase with LRO. At small λ, the critical line increases sharply from $\alpha = 2$ and displays a negative curvature. By contrast, spin-wave theory (see figure 1) and the large N approximation predict that $\alpha_c(\lambda \to 0) = 1$. In the range of λ considered here ($\lambda < 8$), the critical line stays well below the value $\alpha = 3$ and we expect this feature to remain true for all λ. This behaviour is consistent with the proof of absence of LRO at $T = 0$ for $\alpha > 3$ [15] (see footnote 1).

5.3. Critical exponents

The transition line between Néel LRO and QLRO is a non-trivial line which displays continuously varying critical exponents, as we show now.

5.3.1. Divergence of the crossover length scale. The standard theory of quantum phase transitions involves a set of critical exponents which govern the universal behaviour of various quantities close to or at the QCP. One of them is ν, which tells us how the correlation length diverges in the real space direction close to the critical point. Usually this correlation length is defined in the disordered phase by the exponential decay $\sim \exp(-r/\xi)$ of the correlation function associated with the order parameter. In our case, the non ordered regime $\lambda < \lambda_c$ is already critical and thus the correlation length is intrinsically infinite. Nevertheless, the typical length scale ξ_λ which governs the crossover phenomenon diverges at the QCP (on both sides) with an exponent which we call ν by analogy:

$$\xi_\lambda \propto |\lambda - \lambda_c|^{-\nu}. \tag{31}$$

As already discussed, an accurate numerical evaluation of the exponent ν is difficult, because of some intrinsic uncertainties in the data collapse procedure. Nevertheless, at our level of precision we observe this crossover length scale exponent increasing when $\alpha \to 2^+$. In particular, at the marginal point $\alpha = 2$, we find an exponential divergence of ξ_λ near $\lambda = 0$ (equation (30)), formally corresponding to $\nu = \infty$. This divergence of ν when α approaches 2 is actually in good agreement with the results of field theory and RG calculations presented in section 6.

5.3.2. Staggered magnetization exponent and hyperscaling relation. The other scaling parameter Ψ_λ, used for the collapse of the correlation function data, also contains some information. First, if the scaling hypothesis used above with the help of the crossover functions is correct, we expect $\Psi_\lambda \sim \xi_\lambda^{z+\eta-1}$, which gives another estimate for the critical exponent of the decay of the correlation function (equation (27)). This is illustrated in figure 7, where Ψ_λ is plotted versus ξ_λ for $\alpha = 2.1$. Data, presented for both sides of the transition in figure 7, clearly display power-law dependences with an exponent $\eta + z - 1$ in very good agreement with the value of 0.63 previously found along the separatrix in figure 4(b). Note also that the agreement is even better when getting closer to the QCP.

In the ordered phase, according to equation (26), we expect for the AF order parameter

$$m_{\mathrm{AF}} \propto \xi_\lambda^{(1-z-\eta)/2} \propto (\lambda - \lambda_c)^{(\nu(1-z-\eta))/2}. \tag{32}$$

This implies the usual *hyperscaling* relation involving the critical exponent β governing the onset of the order parameter

$$m_{\mathrm{AF}} \propto (\lambda - \lambda_c)^\beta, \tag{33}$$

which must therefore satisfy

$$2\beta = \nu(z + \eta - 1), \tag{34}$$
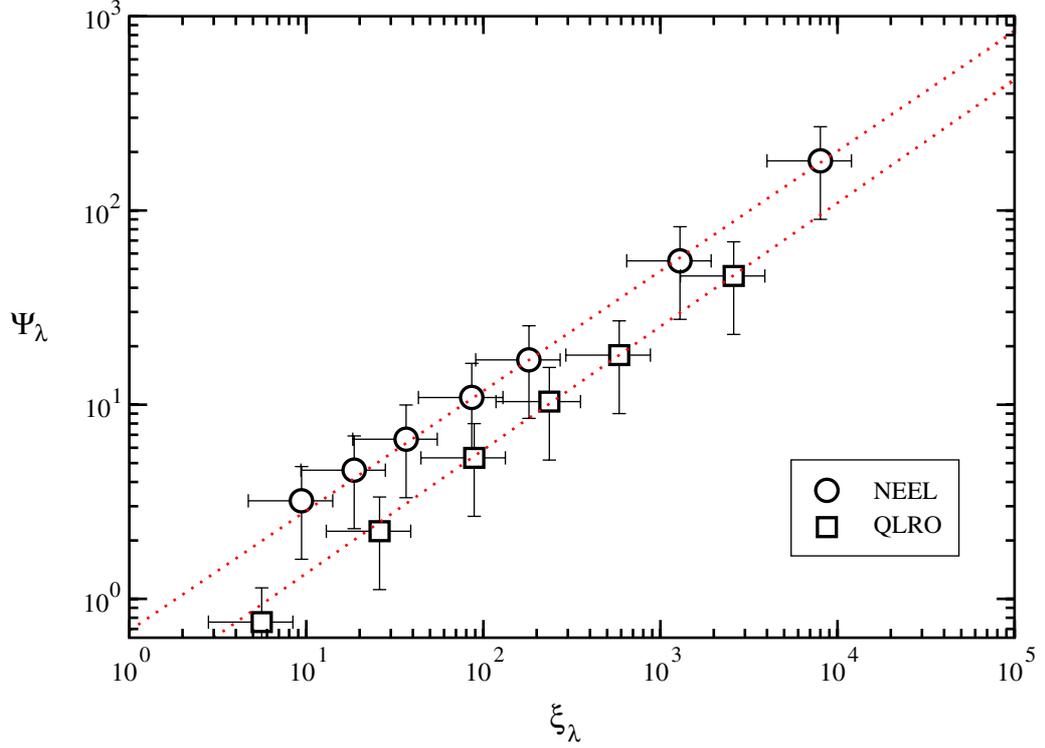
i.e. the usual hyperscaling relation in $d = 1$.

Figure 7. Log–log plot of the scaling parameters Ψ_λ and ξ_λ obtained from the collapses shown in figure 4(b) for $\alpha = 2.1$ in both phases: Néel ($\circ$) and QLRO ($\square$). Within error bars (explicitly shown on the plot), data are fitted by power-laws (dotted lines) of the form $\xi_\lambda^{0.617}$ for the Néel regime and $\xi_\lambda^{0.636}$ for the QLRO.

5.3.3. Analytical estimate of the exponent η. Following the same philosophy as in the mean field argument given in section 2, we can calculate the expectation value of the long range perturbation

$$J(r, r')\langle \vec{S}_r \cdot \vec{S}_{r'} \rangle \sim \frac{1}{|r - r'|^{\alpha + z + \eta - 1}}, \tag{35}$$

at the QCP, with some unknown critical exponents z and η. The finite size correction to the free energy density now scales like $L^{2-\alpha-z-\eta}$. The singular part of the free energy at some non-trivial QCP is expected to scale like L^{-1-z} for a finite size system. Thus the two corrections will scale in a similar way if

$$\eta = 3 - \alpha. \tag{36}$$

The same condition is also obtained by demanding that the long range interaction be invariant under the RG transformation involving a scale factor s:

$$\vec{n}(\tau, x) \rightarrow s^{-(z-1+\eta)/2}\vec{n}(\tau/s^z, x/s). \tag{37}$$

(The rescaling factor of $s^{-(z-1+\eta)/2}$ for $\vec{n}$ implies the equal time correlation exponent of $z - 1 + \eta$.) Rescaling x and τ inside the integral equation (15) (which represents the contribution of the long range term in the action), the condition for invariance under this

RG transformation leads to $2 + z - \alpha - (z - 1 + \eta) = 0$, which gives the expression (36) for η. As already shown in section 3, large N calculations also give the same value for η.[4] Let us mention that the RG analysis, presented below in section 6, also agrees with such an estimate, up to order $(\alpha - 2)^2$.

5.3.4. Numerical determination of the exponent η: scaling of the staggered susceptibility. The $T = 0$ staggered susceptibility, defined on a finite ring of size L by

$$\chi(\pi) = \frac{1}{L} \sum_{ij} (-1)^{|i-j|} \int_0^\infty \langle \vec{S}_i(0) \cdot \vec{S}_j(\tau) \rangle \, \mathrm{d}\tau, \tag{38}$$

obeys the standard finite size scaling at the QCP:

$$\chi(\pi) \propto L^{2-\eta}. \tag{39}$$

Also we know, for instance from SW calculation (see appendix A), that in a Néel ordered state the staggered susceptibility will scale quadratically with the size L. On the other hand, in the QLRO characterized by $\eta = 1$, we rather expect a linear scaling of $\chi(\pi)$ with L. Consequently, there are three distinct regimes for the staggered susceptibility:

$$\chi(\pi) \times L^{-2} \sim \begin{cases} \text{constant} & \text{if } \lambda > \lambda_c \quad \text{(NEEL)} \\ L^{-1} & \text{if } \lambda < \lambda_c \quad \text{(QLRO)} \\ L^{-\eta} & \text{if } \lambda = \lambda_c \quad \text{(QCP)}. \end{cases} \tag{40}$$

We use the same scaling procedure as for the correlation functions, to obtain data collapses onto two different curves, as illustrated in figure 8 for $\alpha = 2.2$. Indeed $\chi(\pi)$, computed with QMC on chains of up to $L = 1000$ sites, displays clearly a crossover phenomenon on both sides of the transition, also characterized by a crossover length scale which is directly proportional to the one previously extracted in the analysis of the correlation functions. Note also that such an analysis provides a second physical observable way to locate the QCP: in fact, the analyses of $C(L)$ and $\chi(\pi)$ both agree (within the error bars) on the value of λ_c. Moreover, we expect the scaling hypothesis to be valid if $\Theta_\lambda \sim \xi_\lambda^\eta$. This is actually the case, as illustrated in the lower inset of figure 8 where we find $\eta = 0.8 \pm 0.015$. We can also obtain the quantum critical exponent η from the separatrix between the Néel and QLRO regimes (see figure 8), which is expected to decay as $L^{-\eta}$. For $\alpha = 2.2$, we find $\eta = 0.8 \pm 0.01$. We have repeated this computation of $\chi(\pi)$ for several other values of $\alpha \in [2.1, 2.7]$ to calculate the corresponding $\eta(\alpha)$. The results are plotted in figure 9, and compared to the previously discussed estimate $\eta = 3 - \alpha$. It is very remarkable to see how this rough estimate reproduces quite well the actual value. Only for $\alpha > 2.3$ a deviation starts to appear.

5.3.5. Dynamical exponent $z < 1$. The dynamical critical exponent z, involved for instance in the critical decay of the correlation function equation (27), can be evaluated from the spin–spin correlation function at the QCP. From the fit of the separatrix

---

[4] It is important to note that, up to small corrections, this estimate equation (36) was also found three decades ago by several authors for the related n-vector model with long range interaction [7, 9, 22].
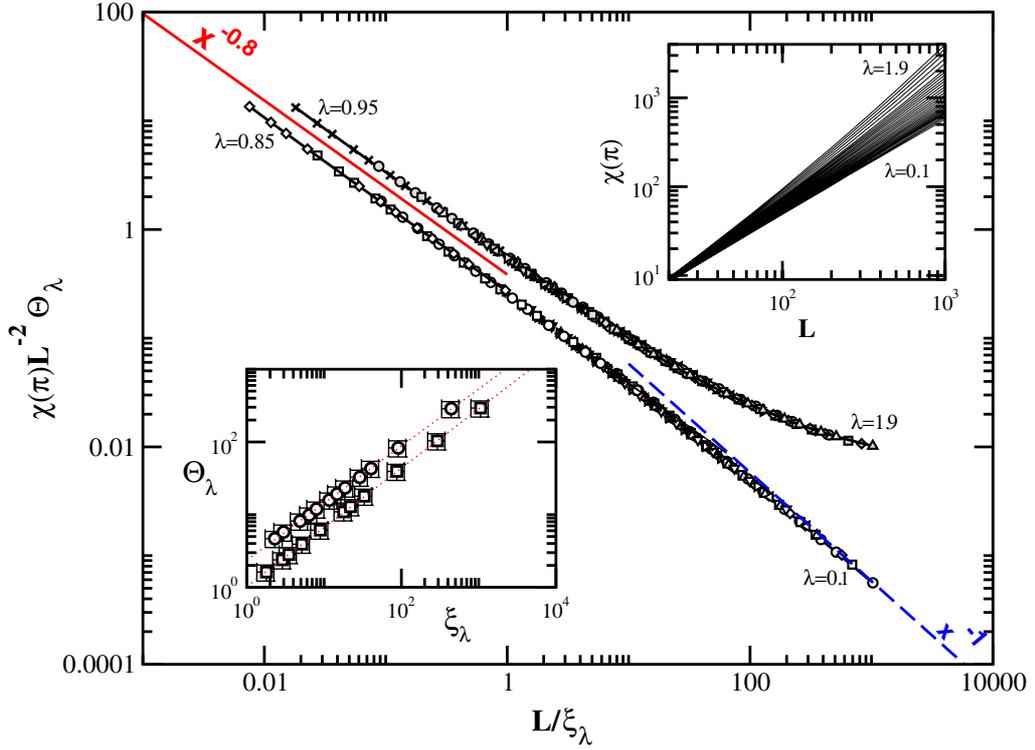
Figure 8. QMC results for the $T = 0$ staggered susceptibility $\chi(\pi)$ (equation (38)) computed for $\alpha = 2.2$ on systems up to $L = 1024$ spins. The upper inset shows $\chi(\pi)$ versus L for various $\lambda \in [0.1, 1.9]$. The main plot shows the results of a data collapse onto two universal curves, after a rescaling of both x- and y-axes using two parameters ξ_λ and Θ_λ. Asymptotically, the LRO curve (top one with data for $0.95 \leq \lambda \leq 1.9$) saturates towards a constant whereas the QLRO one (lower one with data for $0.1 \leq \lambda \leq 0.85$) displays an L^{-1} behaviour, characteristic of $\eta = 1$. Between them the separatrix shows the critical behaviour around the transition at $\lambda_c \simeq 0.9$, decaying like $L^{-0.8 \pm 0.01}$. The lower inset shows a log–log plot of the scaling parameters Θ_λ and ξ_λ used to achieve the collapses in both phases, Néel ($\bigcirc$) and QLRO ($\square$). Within error bars, data can be fitted for the entire range by power laws (dotted lines) of the form $\xi_\lambda^{0.785}$ for the Néel regime and $\xi_\lambda^{0.815}$ for the QLRO.

between the two data collapses (see for instance figure 4 where for $\alpha = 2.1$ we estimated $\eta + z - 1 = 0.63 \pm 0.03$) we obtain an estimate for $\eta + z - 1$. Then, using the estimates of η, determined separately with the staggered susceptibility, we obtain a numerical evaluation of z. Results are shown in figure 10 for $2 \leq \alpha \leq 2.7$. For $\alpha = 2$, the QCP at $\lambda = 0$ displays the critical behaviour of the short range model, with $\eta = z = 1$. Surprisingly, when moving from $\alpha = 2$ along the transition line, z becomes very rapidly <1 and, within the error bars, seems to saturate around a value ~ 0.75. It is actually natural to expect $z \neq 1$ since the long range interaction breaks Lorentz invariance. However, unlike for the estimate of η, the dynamical exponent obtained within the large N expansion $z = (\alpha - 1)/2$ does not agree with the QMC results. As we discuss in the next section, using an 'RG improved' perturbation theory, z is found to be <1 but does not display such a big reduction.
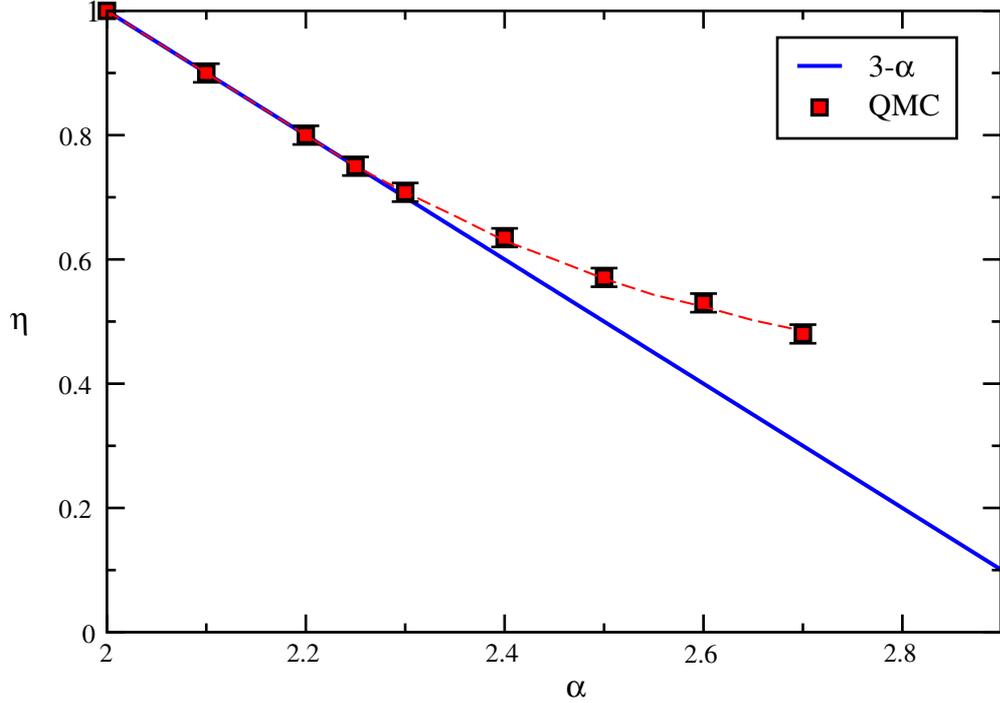
Figure 9. Numerical estimate for the critical exponent η along the critical line obtained using the critical behaviour of $\chi(\pi)$ computed with QMC (red symbols). The red dashed line is a guide to the eyes. The blue full line is the analytical estimate $\eta = 3 - \alpha$.

6. Field theory/renormalization group results

The low energy, continuum limit, imaginary time action takes the form

$$S[\vec{n}] = S_0[\vec{n}] - g \int d\tau \, dx \, \phi(\tau, x) - \lambda a^{\alpha-2} \int \frac{d\tau \, dx \, dy}{|x-y|^\alpha} \vec{n}(\tau, x) \cdot \vec{n}(\tau, y). \quad (41)$$

$\vec{n}(\tau, x)$ is the antiferromagnetic order parameter field defined by the continuum limit expression of equation (13). Here S_0 is the action for a free massless relativistic boson, in terms of which $\vec{n}$ may be represented in a non-linear way. Equivalently, we may regard it as the action of the $k = 1$ Wess–Zumino–Witten non-linear σ model. The field ϕ is defined as

$$\phi = 2\pi \vec{J}_{\mathrm{L}} \cdot \vec{J}_{\mathrm{R}}, \quad (42)$$

and is normalized so

$$\langle \phi(z)\phi(0) \rangle = \frac{3}{16\pi^2 |z|^4}. \quad (43)$$

The corresponding coupling constant, g, has a bare value of order unity for the short range AF chain and is marginally irrelevant. It is responsible for various logarithmic corrections such as the one in the correlation function of equation (3). Note that the dimensionless coupling constant for the long range interaction λ is only proportional to the one used
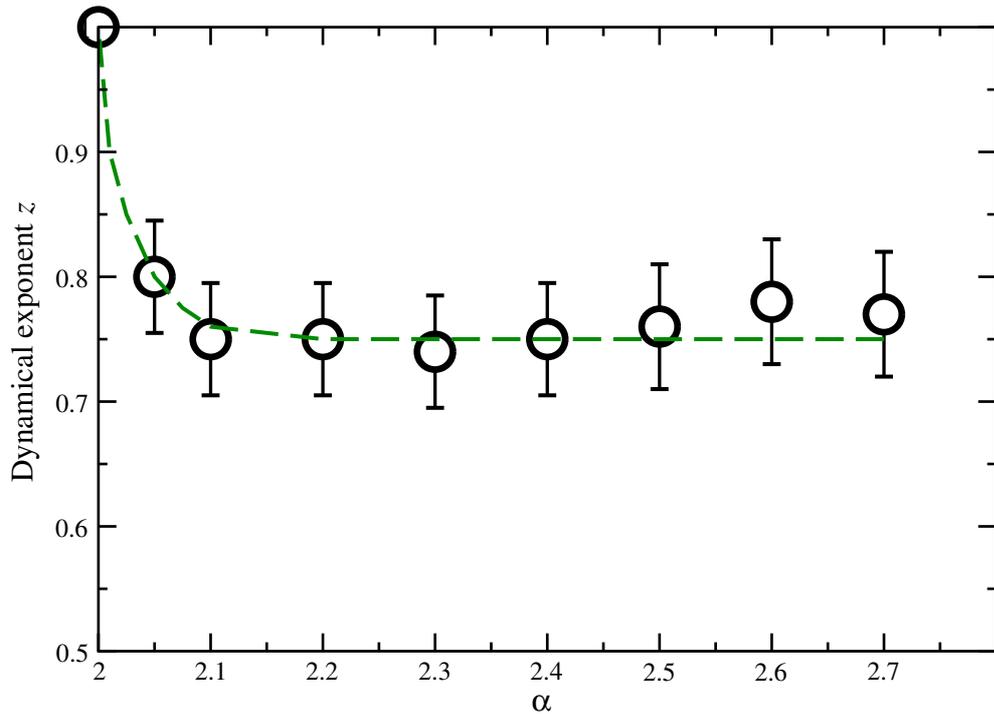
Figure 10. Numerical estimates for the dynamical critical exponent z along the critical line obtained using the critical behaviour of the correlation function (equation (27)) computed with QMC, and the numerical estimate of η (see figure 9). The numerical results (open circles) suffer from large error bars, as shown on the plot. The green dashed line is a guide to the eyes.

before for the lattice microscopic model in equation (4), and a is a short distance cut-off with dimensions of length. As already noted in section 2, since $\vec{n}$ has a scaling dimension of $1/2$ from equation (14), λ is irrelevant for $\alpha > 2$, relevant for $\alpha < 2$, and marginal for $\alpha = 2$. Also note that $\lambda > 0$ corresponds to non-frustrating interactions which favour the Néel state where $\langle n^z \rangle \neq 0$. Our strategy is to study this model when $0 < \alpha - 2 \ll 1$ and $0 < \lambda \ll 1$ using perturbation theory in g and λ. Since g renormalizes to zero at large length scales, when $\lambda = 0$ (i.e. in the short range model) this can give useful results, for small bare λ, even when the bare value of g is O(1). We will find that an interplay between the local marginal coupling constant g and the irrelevant non-local coupling constant λ governs the critical behaviour in this regime.

We now consider the low energy effective field theory for the long range model in equation (41), in the limit of small g and λ, using RG methods. When $\lambda = 0$, the RG equations reduce to the standard ones for the short range model. These take the form

$$\frac{\mathrm{d}g}{\mathrm{d}\ln a} = -g^2 - (1/2)g^3 + \cdots. \tag{44}$$

Here we define our RG transformation by increasing the short distance cut-off a. The bare value of g is positive for any non-frustrated short range model and is typically O(1). The basin of attraction of the $g = 0$ fixed point is known to extend to such large bare values of g so that $g = 0$ is the universal stable fixed point for short range models. The flow of

g towards zero at long length scales is controlled by the quadratic term in the β-function of equation (44), giving

$$g(a) \to \frac{1}{\ln(a/a_0)}, \tag{45}$$

where a_0 is the original cut-off and a is a larger value obtained from integrating out modes with wavelengths between a_0 and a. This logarithmically slow flow of $g(a)$ to zero is responsible for logarithmic corrections to the correlation function and other properties of the short range models. A linear term in the β-function for λ follows immediately from the factor of $a^{\alpha-2}$ in equation (41), which in turn is a consequence of the fact that n has scaling dimension $1/2$:

$$\frac{\mathrm{d}\lambda}{\mathrm{d}\ln a} = (2-\alpha)\lambda + \cdots. \tag{46}$$

So, ignoring the effects of g, λ grows larger at long length scales for $\alpha < 2$ but smaller for $\alpha > 2$. Long range interactions are irrelevant for $\alpha > 2$. However, it is necessary to consider higher order terms in the β-functions for both g and λ to understand the phase diagram, even at $\alpha \approx 2$.

To calculate additional terms in the β-functions, we define our ultra-violet cut-off by forbidding any two points in space-imaginary time from getting closer than a, in a perturbative calculation of the partition function (or long distance Green's functions). In particular, this means that the long range term in the action is cut off as

$$S_\lambda = -\lambda a^{\alpha-2} \int_{|x-y|>a} \frac{\mathrm{d}\tau\,\mathrm{d}x\,\mathrm{d}y}{|x-y|^\alpha} \vec{n}(\tau,x) \cdot \vec{n}(\tau,y). \tag{47}$$

When the cut-off is increased from a_0 to $a = a_0 + \delta a$, there is an additional change in S of first order in δa, which comes from the change in the integration region:

$$\delta S = -\lambda a_0^{\alpha-2} \int \mathrm{d}x\,\mathrm{d}\tau \left[\int_{-a}^{-a_0} + \int_{a_0}^{a} \right] \frac{\mathrm{d}u}{|u|^\alpha} \vec{n}(\tau,x) \cdot \vec{n}(\tau,x+u). \tag{48}$$

Since both factors of $\vec{n}$ are very close together, we may use the operator product expansion. This follows from the three-point Green's function:

$$\langle n^a(z_1)\phi(z_2)n^b(z_3) \rangle = \frac{1}{8\pi} \frac{|z_{13}|}{|z_{12}|^2 |z_{23}|^2}. \tag{49}$$

This implies the operator product expansion (OPE):

$$n^a(z)n^b(0) \to \frac{\delta^{ab}2\pi}{3} |z|\phi(0) + \cdots. \tag{50}$$

Using this in equation (48) gives

$$\delta S = -\lambda a_0^{\alpha-2} \int \mathrm{d}\tau\,\mathrm{d}x\,\phi(\tau,x)4\pi \int_{a_0}^{a} \frac{\mathrm{d}u}{|u|^{\alpha-1}} \approx -\frac{\delta a}{a}4\pi\lambda \int \mathrm{d}\tau\,\mathrm{d}x\,\phi(\tau,x). \tag{51}$$

This corresponds to a renormalization of g,

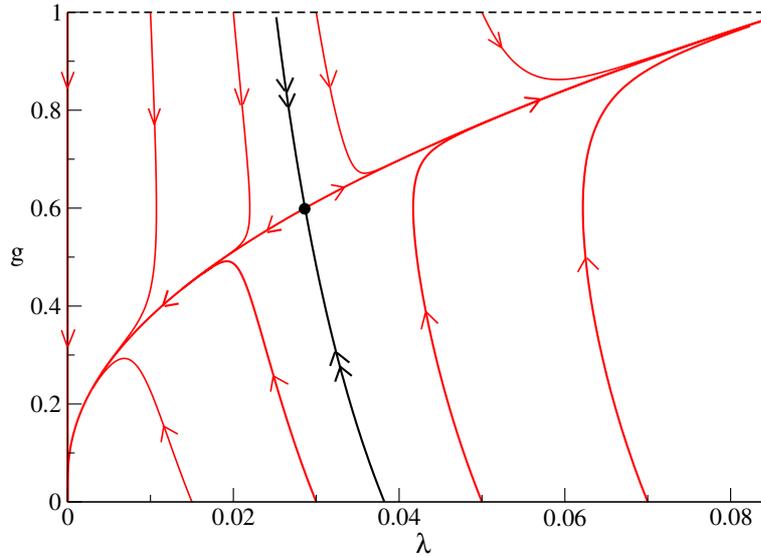$$\delta g = 4\pi\frac{\delta a}{a}\lambda \tag{52}$$

Figure 11. Renormalization group flow of equations (53) and (55) in the case $\alpha = 2.3$. The dotted line represents, schematically, the values of the bare couplings in the field theory as the parameter λ in the lattice model is varied. The unstable fixed point at $\lambda_c = 0.0286$, $g_c = 0.6$ separates the flow to the stable fixed point at $\lambda = g = 0$ which represents the quasi-long-range ordered phase and the flow to infinite λ, g, which represents the long range ordered phase. The black lines with double arrows denote the separatrixes between these two phases. (The corrections to the flow equations are presumably significant for this large a value of $\alpha - 2$, but we graph this case for ease of visualization.)

and hence to another term in the β-function for g:

$$\frac{\mathrm{d}g}{\mathrm{d}\ln a} = 4\pi\lambda - g^2 + \cdots. \tag{53}$$

There is one more term in the RG equations that is important at small $\alpha-2$, corresponding to a correction to λ of order λg. This can be calculated from the OPE:

$$\phi(z)n^a(0) \to \frac{1}{8\pi|z|^2}n^a(0) + \cdots, \tag{54}$$

giving

$$\mathrm{d}\lambda/\mathrm{d}\ln a = -(\alpha - 2)\lambda + (1/2)\lambda g + \cdots. \tag{55}$$

The RG equations, equations (53) and (55), have an unstable fixed point for $\alpha > 2$, at

$$\begin{aligned} g_c &\approx 2(\alpha - 2) \\ \lambda_c &\approx \frac{1}{\pi}(\alpha - 2)^2. \end{aligned} \tag{56}$$

For $\alpha < 2$, a positive λ always runs away to large values as we lower the cut-off (i.e. increase a), corresponding to LRO. On the other hand, for $\alpha > 2$, a small enough positive bare λ flows to zero while a larger bare value flows to large values (see figure 11). These

statements remain true even when the bare value of g is O(1) as we expect it to be in general for a short range spin chain. For a small bare λ, g initially renormalizes towards small values as it would in the short range chain until eventually equations (53), (55) becomes valid. The stable $\lambda = g = 0$ fixed points correspond to the standard QLRO phase of the short range spin chain. The non-trivial unstable fixed point separates the ordered and quasi-long-range ordered phases. Of course, there are higher order terms in both RG equations, but they do not invalidate our conclusions on the location of the fixed point, for small enough $\alpha - 2$. Both terms on the right-hand side of equation (53) are $\mathrm{O}[(\alpha - 2)^2]$ at the fixed point; any possible higher order terms such as g^3 or λ^4 are at least of $\mathrm{O}[(\alpha - 2)^3]$. Similarly, both terms on the right-hand side of equation (55) are $\mathrm{O}[(\alpha - 2)^3]$ at the fixed point; higher order terms are at least $\mathrm{O}[(\alpha - 2)^4]$. To reach this conclusion it is important to realize that there cannot be any terms in $\mathrm{d}\lambda/\mathrm{d}\ln a$ which contain no factors of λ; a purely short range interaction cannot generate a long range one, although the reverse is not true.

Thus we appear to have a rare example of a non-trivial fixed point which can be accessed perturbatively. (But see the discussion below of potential problems with this approach.) We note that a similar expansion for long range classical spin models was introduced in [7]. See also [23, 24]. Our quantum spin model, in the continuum limit, non-linear σ model approximation, appears rather similar, in the imaginary time path integral formulation. An important difference, however, is that our model has an action which is long range in the space direction but short range in the time direction. Thus it corresponds to a classical model in two space dimensions with short range interactions in one direction and long range interactions in the other. It is this asymmetry which leads to a dynamical critical exponent $z < 1$. Another important difference from a two-dimensional Heisenberg model is the topological term in the short range part of the action which is responsible for the quasi-long-range order. We remark that an integer-spin quantum Heisenberg chain with long range interactions could be expected to have identical critical behaviour to a classical Heisenberg model in two dimensions with interactions which are long range in one dimension. We also remark that an xxz quantum spin chain with long range interactions could be expected to have the same critical behaviour as a two-dimensional classical xy model with interactions which are long range in one dimension.

The phase boundary (or separatrix) can be found by determining the line in the g–λ plane which renormalizes to the critical point. Combining equations (53) and (55) gives

$$\int_{\lambda_0}^{\lambda_\mathrm{c}} \frac{\mathrm{d}\lambda}{\lambda} = (1/2) \int_{g_\mathrm{c}}^{g_0} \frac{\mathrm{d}g(g - g_\mathrm{c})}{g^2 - g_\mathrm{c}^2(\lambda/\lambda_\mathrm{c})}, \tag{57}$$

where $\lambda = \lambda(g)$ is a function of g along the RG flow in the integral on the right-hand side of equation (57). g_0 and λ_0 are the values at arbitrary points on the separatrix. Since λ increases monotonically to the value λ_c with increasing a, we may obtain an upper and lower bound on the right-hand side by replacing $\lambda(g)$ by λ_c and zero respectively inside the integral on the right-hand side of equation (57):

$$(1/2)\ln(g_0/eg_\mathrm{c}) + g_\mathrm{c}/2g_0 < \ln(\lambda_\mathrm{c}/\lambda_0) < (1/2)\ln[(g_0 + g_\mathrm{c})/2g_\mathrm{c}]. \tag{58}$$

Now using the fact that $g_\mathrm{c} \ll g_0$, this becomes

$$\sqrt{g_0/eg_\mathrm{c}} < \lambda_\mathrm{c}/\lambda_0 < \sqrt{g_0/2g_\mathrm{c}}, \tag{59}$$
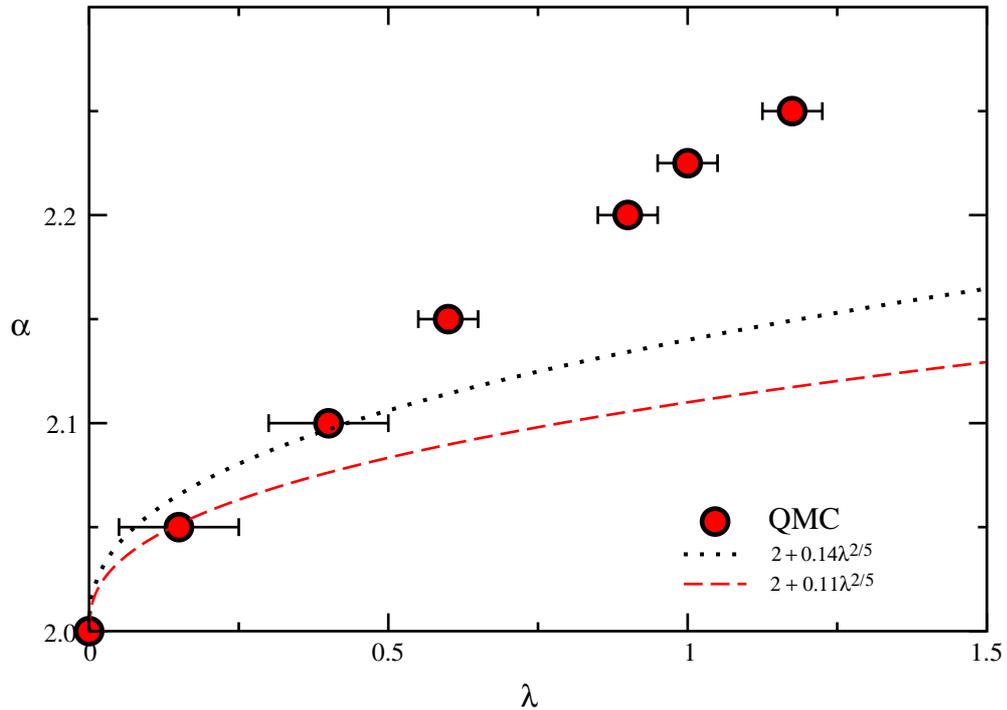
Figure 12. QMC phase diagram at small λ compared to the RG prediction of equation (61) with $C = 0.14$ and 0.11.

that is

$$0.637(\alpha - 2)^{5/2}/\sqrt{g_0} < \lambda_0 < 0.743(\alpha - 2)^{5/2}/\sqrt{g_0}. \tag{60}$$

Thus on the separatrix λ_0 is $O[(\alpha - 2)^{5/2}]$. (A numerical solution of the RG equations indicates that λ_0 is very close to the lower bound in equation (60).) Assuming a bare g of $O(1)$, it is then possible to predict the shape of the phase boundary in the λ–α plane close to $\alpha = 2$. There is an unknown multiplicative factor relating the lattice coupling λ to the continuum coupling λ. However, we can predict that

$$\alpha_c(\lambda) \to 2 + C\lambda^{2/5}, \tag{61}$$

for some unknown constant factor, C, as $\alpha \to 2$. As mentioned above, we expect that $2 < \alpha_c(\lambda) < 3$ for all λ and all S. While our QMC results also predict that $\alpha_c \to 2$ when $\lambda \to 0$, but otherwise equation (61) does not agree well with the QMC result as shown in figure 12. It is interesting to note that lowest order SW theory and the large N approximation make the mean-field prediction that $\alpha_c \to 1$ as $\lambda \to 0$, in clear disagreement with our RG and QMC results.

Linearizing the β-functions at the critical point gives

$$\frac{\mathrm{d}}{\mathrm{d}\ln a}\begin{pmatrix} \lambda - \lambda_c \\ g - g_c \end{pmatrix} \approx \begin{pmatrix} 0 & (\alpha - 2)^2/(2\pi) \\ 4\pi & -4(\alpha - 2) \end{pmatrix}\begin{pmatrix} \lambda - \lambda_c \\ g - g_c \end{pmatrix}. \tag{62}$$

This matrix has one positive (unstable) right eigenvalue, $(\sqrt{6} - 2)(\alpha - 2)$, implying a crossover length scale

$$\xi \propto |\lambda - \lambda_{\mathrm{c}}|^{-\nu}, \tag{63}$$

with a critical exponent

$$\nu = \frac{1}{(\sqrt{6} - 2)(\alpha - 2)}, \tag{64}$$

which diverges as $\alpha \to 2$. The corresponding unstable direction is

$$\lambda - \lambda_{\mathrm{c}} = \frac{(\alpha - 2)}{2\pi(\sqrt{6} - 2)}(g - g_{\mathrm{c}}). \tag{65}$$

For $\alpha = 2$ exactly, LRO occurs for any $\lambda > 0$ but behaviour characteristic of the quasi-long-range ordered fixed point occurs out to a cross over length scale:

$$\xi \propto \exp[C/\lambda_0^{2/5}], \tag{66}$$

for a constant factor C.

We may also determine the critical exponent, $\eta + z - 1$, controlling the equal-time correlation function at the non-trivial critical exponent:

$$\langle S_0^a S_j^b \rangle \propto \frac{\delta^{ab}}{|j|^{\eta + z - 1}}, \tag{67}$$

when $\alpha - 2 \ll 1$. Since λ and g are both small at the critical point, for $\alpha - 2 \ll 1$, we may simply use 'RG improved' perturbation theory. That is, we calculate the correlation function to first order perturbation theory in g, replace g by g_{c}, and interpret the result as the expression equation (67) with

$$\eta + z = 2 + \mathrm{O}(g_{\mathrm{c}}). \tag{68}$$

(To lowest order in $(\alpha - 2)$ we only need consider g, not λ, since $\lambda_{\mathrm{c}} \propto g_{\mathrm{c}}^2$.) The Green's function, up to first order in perturbation theory in g, the bare coupling, is

$$\begin{aligned}
\langle n^a(z)n^b(0) \rangle &= \frac{\delta^{ab}}{|z|} + g \int \mathrm{d}^2 z' \langle n^a(z)n^b(0)\phi(z') \rangle \\
&= \frac{\delta^{ab}}{|z|} + \frac{g}{2\sqrt{3}}\delta^{ab} \int \mathrm{d}^2 z' \frac{|z|}{|z'|^2|z - z'|^2} + \cdots.
\end{aligned} \tag{69}$$

The integral in equation (69) must be restricted to the region $|z'| > a$, $|z - z'| > a$. For $|z| \gg a$, the integral is dominated by the two regions, $|z'| \ll |z|$ and $|z' - z| \ll |z|$, giving

$$\begin{aligned}
\langle n^a(z)n^b(0) \rangle &\approx \frac{\delta^{ab}}{|z|} \left[1 + \frac{g}{2\sqrt{3}} 2 \int \frac{\mathrm{d}^2 z'}{|z'|^2} \right] \\
&\approx \frac{\delta^{ab}}{|z|} \left[1 + \frac{g}{2\sqrt{3}} 4\pi \ln(|z|/a) \right].
\end{aligned} \tag{70}$$

Now replacing g by g_{c}, its fixed point value, we obtain

$$\langle n^a(z)n^b(0) \rangle = \frac{\delta^{ab}}{|z|} \left\{ 1 + (\alpha - 2)\ln(|z|/a) + O[(\alpha - 2)^2] \right\}. \tag{71}$$

Now, using the fact that the correlation function should have a pure power-law form at the fixed point, we may interpret this result as the leading term in the expansion of

$$\langle n^a(z)n^b(0)\rangle = \frac{\delta^{ab}A}{|z|^{1-(\alpha-2)}}. \tag{72}$$

To this order in $(\alpha - 2)$ we obtain the same exponent for $z = \mathrm{i}x$ or $z = \tau$, implying that the corrections to the dynamical exponent, $z = 1$, are higher order in $(\alpha - 2)$. Thus

$$\eta = 1 - (\alpha - 2) + \mathrm{O}[(\alpha - 2)^2]. \tag{73}$$

This is the same value of η as found in the large N approximation and by a simple scaling argument in section 5.3.3. It agrees well with QMC results for $\alpha < 2.3$ as shown in figure 9. It is natural to expect that $z \neq 1$ since the long range interaction breaks Lorentz invariance. Since $\omega \propto |k|^{(\alpha-1)/2}$ in the ordered phase it is natural to expect that $z < 1$ at the critical point, as is found in the large N approximation. However, clearly $1 - z$ must be at least $\mathrm{O}[(\alpha - 2)^2]$ since the long range coupling constant, λ, is of that order. In fact, we suspect that $1 - z$ is even higher order than quadratic in $(\alpha - 2)$. This conclusion does not fit well with the QMC results for z, presented in figure 10. There it was found (although with large error bars) that z appears to have a nearly constant value, $z \approx 0.75$, for $\alpha \geq 2.1$. As α is further decreased z appears to rise very rapidly towards unity.

So far, we have ignored another possible interaction:

$$S \to S - (g'\pi/3) \int \mathrm{d}\tau\, \mathrm{d}x(\vec{J}_\mathrm{L}^2 + \vec{J}_\mathrm{R}^2). \tag{74}$$

This interaction is, in fact, present for the short range spin-chain with a large coefficient. Since the Hamiltonian for the $k = 1$ WZW model can be written quadratic in currents, this 'interaction' term can be regarded as simply shifting the velocity, which we have so far set equal to unity, to

$$v \to 1 - g'/2. \tag{75}$$

The RG equations for the short range model, including g', take the form, to cubic order,

$$\frac{\mathrm{d}g}{\mathrm{d}\ln a} = -g^2 - (1/2)g(g^2 + g'^2) \tag{76}$$

$$\frac{\mathrm{d}g'}{\mathrm{d}\ln a} = (3/4)g^3. \tag{77}$$

Starting with g, $g' > 0$ and O(1), these equations predict that $g \to 0$ and g' flows to a value of O(1). The large value of g' at the fixed point can simply be interpreted as a large renormalization of the velocity, provided that $g' < 2$. In fact, this is what happens, for example in the Hubbard model at half-filling. The spin velocity is reduced by the Hubbard interactions. An alternative approach is to adjust v to the correct value and drop g' completely from the RG equations. In fact, equation (77) depends strongly on the renormalization and cut-off scheme. With a Lorentz invariant cut-off and renormalization procedure, the non-Lorentz-invariant term, proportional to g', will not be generated under the RG if it is initially absent. Breaking of Lorentz invariance in this problem at low energies just means shifting the velocity. If we work directly with the exact velocity, then it is apparently permissible to set $g' = 0$ and use a Lorentz invariant renormalization

procedure so that g' remains zero under renormalization. In fact, using this procedure in equation (76) leads to various predictions of logarithmic corrections which are in good agreement with the Bethe ansatz and numerical results for the $S = 1/2$ chain. If we set g' equal to some arbitrary non-zero value in equation (76) the coefficients and powers of log corrections would change, resulting in worse agreements with numerical results. Thus, this procedure of ignoring g' seems to be a valid and useful one.

We now consider the interplay of the long range coupling constant, λ, with the non-Lorentz invariant local coupling, g'. The needed OPEs can be obtained from the general conformal field theory result for the three-point Green's function of the energy momentum operator with a primary field of left-dimension 1/4:

$$\langle T(z)n^a(z_1)n^b(z_2)\rangle = \frac{1}{2\pi}\sum_{i=1}^{2}\left[\frac{1/4}{(z-z_i)^2}+\frac{1}{z-z_i}\frac{\partial}{\partial z_i}\right]\frac{\delta^{ab}}{|z_1-z_2|}. \tag{78}$$

Here $T = (2\pi/3)\vec{J}_{\mathrm{L}}^2$ is the left-moving part of the Hamiltonian. This gives

$$\langle T(z)n^a(z_1)n^b(z_2)\rangle = \frac{1}{8\pi}\frac{\delta^{ab}(z_1-z_2)^2}{|z_1-z_2|(z-z_1)^2(z-z_2)^2}. \tag{79}$$

Also using the two-point function of T,

$$\langle T(z_1)T(z_2)\rangle = \frac{1}{2(2\pi)^2(z_1-z_2)^4}, \tag{80}$$

we can deduce the OPE:

$$n^a(z)n^b(0) \to \frac{\delta^{ab}\pi z^2}{|z|}T(0). \tag{81}$$

Now consider the case where the separation is in the space direction, $z = \mathrm{i}x$,

$$n^a(x)n^b(0) \to \delta^{ab}\pi|x|[(2/3)\phi(0) - T(0) - \bar{T}(0)] + \cdots. \tag{82}$$

Here we have included the identical OPE coefficient for $\bar{T} \equiv (2\pi/3)\vec{J}_{\mathrm{R}}^2$ and also the coefficient deduced earlier, in equation (50). Using the same cut-off and RG transformation procedure as above, this implies a term in the β-function:

$$\frac{\mathrm{d}g'}{\mathrm{d}\ln a} = -6\pi\lambda. \tag{83}$$

This drives g' towards negative values, corresponding to increasing the velocity. If we continue to use our previous RG transformation, we find that the $\mathrm{d}\lambda/\mathrm{d}\ln a$ *does not* pick up a term $\propto\lambda g'$. The difference from the non-zero λg term in equation (86) arises from the fact that the OPE is now

$$T(z)n^a(0) \to \frac{1}{8\pi z^2}n^a(0). \tag{84}$$

The RG transformation gives

$$\delta\lambda \propto \int\frac{\mathrm{d}^2z}{z^2}, \tag{85}$$

where, as before, the integral is over a circular shell with radius between a and $a + \delta a$. This integral vanishes by rotational invariance. Thus the complete set of RG equations to low order is

$$
\begin{aligned}
\frac{\mathrm{d}\lambda}{\mathrm{d}\ln a} &= -(\alpha - 2)\lambda + \lambda g/2 \\
\frac{\mathrm{d}g}{\mathrm{d}\ln a} &= 4\pi\lambda - g^2 - (g + g')g^2/2 \\
\frac{\mathrm{d}g'}{\mathrm{d}\ln a} &= -6\pi\lambda.
\end{aligned}
\tag{86}
$$

These equations have an unstable fixed point at

$$
\begin{aligned}
\lambda_{\mathrm{c}} &= 0 \\
g_{\mathrm{c}} &= 2(\alpha - 2) \\
g'_{\mathrm{c}} &= -2 - 2(\alpha - 2) \approx -2.
\end{aligned}
\tag{87}
$$

In this approximation, we obtain the same prediction for $\eta \approx 1 - (\alpha - 2)$ as before and still get $z \approx 1$. There is a shift in the velocity of O(1).

The large value of g' at the fixed point makes the predictions of this RG analysis intrinsically suspect. As in the short range case, we might agree to set v equal to its renormalized value and then drop g' from the RG equations. This leads to the same predictions about the value of λ on the separatrix and ν as obtained above.

However, there are some worrisome features of this RG analysis which arise from the long range interaction. We expect a dynamical exponent $z < 1$ at the critical point. It then does not make sense to use a rotationally invariant (i.e. Lorentz invariant) RG transformation. We would then get back a g^3 term in $\mathrm{d}g'/\mathrm{d}\ln a$ and, very importantly, a $\lambda g'$ term in $\mathrm{d}\lambda/\mathrm{d}\ln a$. We would then generally find that g is not small, O($\alpha - 2$), at the fixed point. λ would also not be small at the fixed point. In this case we would lose all perturbative control over the critical behaviour even for α only slightly larger than 2. In this case, the unstable critical point would not be close to the QLRO fixed point, for α close to 2. One possibility is that the effects associated with $z < 1$ can be ignored to lowest non-trivial order $\alpha - 2$. Then our use of a Lorentz invariant RG transformation may be justified. In this case, the fixed point really is close to the QLRO critical point for α sightly larger than two and our predictions for η and ν are correct in this limit.

The QMC results seem to give at least partial confirmation of the validity of an RG approach based on the $\alpha - 2$ expansion. Most importantly, $\alpha_{\mathrm{c}} \to 2$ as $\lambda \to 0$ and the critical exponents η and z appear to approach their values in the quasi-long-range ordered phase ($\eta = z = 1$) in this limit, with ν diverging. Furthermore, excellent agreement with the prediction for η was obtained, over a rather large range of α (up to 2.2), as shown in figure 9. We were not able to obtain accurate estimates of ν from QMC to test the RG prediction. On the other hand, z showed rather surprising behaviour, in figure 10, dropping rapidly from 1 to about 0.75 as α is increased from 2 to 2.1. This suggests that the asymptotic, small $\alpha - 2$ behaviour may only occur for very small values of $\alpha - 2 \ll 0.1$. Numerical difficulties preclude obtaining QMC data in this region. Furthermore, the phase boundary as determined by QMC, $\alpha_{\mathrm{c}}(\lambda)$, could not be fitted well to the RG prediction of equation (61), except possibly at very small α_{c} (where we have no data) as seen in figure 12. This could be interpreted as meaning that our RG approach based on an

$\alpha - 2$ expansion is correct in principle but is only valid in practice for extremely small values of $\alpha - 2$. (The good agreement for η then appears fortuitous.) Alternatively, the discrepancies may indicate a problem with our RG approach, perhaps resulting from our cavalier treatment of the non-Lorentz-invariant interaction in equation (74).

7. Conclusions

We have studied long range non-frustrating $S = 1/2$ antiferromagnetic chains using spin-wave theory, the large N approximation, quantum Monte Carlo and analytic renormalization group methods based on an expansion in $\alpha - 2$. All methods predict a line of critical points in the λ–α plane with continuously varying critical exponents. This critical line separates phases with true Néel long range order and quasi-long-range order. Quantum Monte Carlo and renormalization group methods indicate that this critical line terminates at $\lambda = 0$, $\alpha = 2$ and suggest that, along the critical line as $\alpha \to 2^+$, $\eta \approx 3 - \alpha$, while ν diverges and $z \to 1^-$.

Acknowledgments

Appendix A. Calculation of finite size corrections from SW: contributions from the $k = 0$ and finite k modes

A.1. General method

Let $\mathcal{H}(h) = \mathcal{H} - h\hat{O}$, where $\hat{O}$ is an operator and h is a field. If we denote by $|h\rangle$ the GS of $\mathcal{H}(h)$, it follows that the GS energy is $E_{\mathrm{GS}}(h) = \langle h|\mathcal{H} - h\hat{O}|h\rangle$. Since $\langle h|h\rangle = 1$, it is straightforward to show (in direct analogy to Feynman's theorem) that

$$\langle \hat{O} \rangle = \langle h|\hat{O}|h\rangle = -\frac{\partial E_{\mathrm{GS}}(h)}{\partial h}. \tag{A.1}$$

In general we need the expectation values of various operators $\hat{O}$ in the unperturbed GS, i.e. in the limit $h \to 0$. It follows that all we have to do is to compute the change in the ground-state energy, due to the perturbation $-h\hat{O}$, to first order in h.

In the remainder of this appendix, the Hamiltonian $\mathcal{H}$ is that of equation (4). We are interested in finite-size chains with an even number of sites L, and periodic boundary conditions.

A.2. Staggered susceptibility

Let $\hat{O} = \sum_i (-1)^i S_i^z$. Then, according to equation (A.1), the staggered magnetization at $T = 0$ is

$$M_\pi = \left\langle \sum_i (-1)^i S_i^z \right\rangle = -\left. \frac{\mathrm{d}E_{\mathrm{GS}}}{\mathrm{d}h} \right|_{h \to 0}$$

and therefore the staggered susceptibility is

$$\chi(\pi) = \frac{1}{L} \left.\frac{\mathrm{d}M_\pi}{\mathrm{d}h}\right|_{h\to 0} = -\frac{1}{L} \left.\frac{\mathrm{d}^2 E_{\mathrm{GS}}}{dh^2}\right|_{h\to 0}.$$

A.2.1. The $k = 0$ contribution. We Fourier transform the spin operators, $\vec{S}_{2n} = 2/L \sum_k \exp(\mathrm{i}k(2na))\vec{S}_k^e$, $\vec{S}_{2n+1} = 2/L \sum_k \exp(\mathrm{i}k(2n+1)a))\vec{S}_k^o$, and collect only the $k = 0$ components. Let us denote by $\vec{S}_1 = \vec{S}_{k=0}^e = \sum_n \vec{S}_{2n}$ and $\vec{S}_2 = \vec{S}_{k=0}^o = \sum_n \vec{S}_{2n+1}$ the total spins of the two magnetic sublattices, of $L/2$ spins each. Since we are in a Néel ordered state, $\vec{S}_1$ and $\vec{S}_2$ are spins of total magnitude $S_L = LS/2 = L/4$ for spins $S = 1/2$. Then, up to some constants that do not depend on h,

$$\mathcal{H}_{k=0}(h) = \mathcal{H}_{k=0} - \mathcal{H}_1 \tag{A.2}$$

where

$$\mathcal{H}_{k=0} = j\vec{S}_1 \cdot \vec{S}_2, \tag{A.3}$$

$$\mathcal{H}_1 = h\left(S_1^z - S_2^z\right) \tag{A.4}$$

and

$$j = \frac{2}{L}\left[1 + \lambda \sum_{n\geq 1} \frac{1}{(2n+1)^\alpha}\right] = \frac{2J_{\mathrm{eff}}}{L}. \tag{A.5}$$

We need to use perturbation theory to second order in h, to find the staggered susceptibility. The ground state of $\mathcal{H}_{k=0}$ is the state

$$|0\rangle = |S_T = 0, M_T = 0, S_L, S_L\rangle = \frac{1}{\sqrt{2S_L + 1}} \sum_{m=-S_L}^{S_L} (-1)^m |m, -m\rangle \tag{A.6}$$

where $\vec{S}_T = \vec{S}_1 + \vec{S}_2$. The perturbation links this only to other states with $M_T = 0$ (see below). Let us denote

$$|S_T\rangle = |S_T, 0, S_L, S_L\rangle \tag{A.7}$$

where $S_T = 0, 1, \ldots, 2S_L$. With this notation, the second-order correction to the ground-state energy is

$$\Delta E_{\mathrm{GS}}^{(2)} = \sum_{n=1}^{2S_L} \frac{|\langle n|\mathcal{H}_1|0\rangle|^2}{E_0 - E_n}. \tag{A.8}$$

However,

$$\mathcal{H}_1|0\rangle = \frac{2h}{\sqrt{2S_L + 1}} \sum_{m=-S_L}^{S_L} (-1)^m m|m, -m\rangle. \tag{A.9}$$

Interestingly enough, one can show that

$$|1\rangle = \alpha_1 \sum_{m=-S_L}^{S_L} (-1)^m m|m, -m\rangle \tag{A.10}$$

where the normalization constant is

$$\alpha_1 = \sqrt{\frac{3}{S_L(S_L+1)(2S_L+1)}}. \tag{A.11}$$

It follows that

$$\langle 1|\mathcal{H}_1|0\rangle = \frac{2h}{\sqrt{2S_L+1}\alpha_1} \tag{A.12}$$

and $\langle n|\mathcal{H}_1|0\rangle = 0$, $\forall n \geq 2$. By direct calculation, we find

$$E_0 = -jS_L(S_L+1); \qquad E_1 = j - jS_L(S_L+1) \tag{A.13}$$

and therefore

$$\Delta E_{\text{GS}}^{(2)} = \frac{|\langle 1|\mathcal{H}_1|0\rangle|^2}{E_0 - E_1} = -\frac{4h^2}{(2S_L+1)\alpha_1^2 j} = -\frac{4h^2}{3j}S_L(S_L+1). \tag{A.14}$$

Since $j = 2J_{\text{eff}}/L$, $S_L = LS/2$, we find

$$\Delta E_{\text{GS}}^{(2)} = -\frac{h^2}{3J_{\text{eff}}}L^2 S\left(\frac{L}{2}S+1\right). \tag{A.15}$$

As a result, the contribution of the $k = 0$ modes to the staggered susceptibility is

$$\chi_{k=0}(\pi) = -\frac{1}{L}\left.\frac{\mathrm{d}^2 E_{\text{GS}}}{\mathrm{d}h^2}\right|_{h=0} = \frac{2}{3}\frac{LS}{J_{\text{eff}}}\left(\frac{L}{2}S+1\right) \sim L^2. \tag{A.16}$$

A.2.2. The contribution of finite k modes. Within the spin-wave approximation, the contribution of the $k \neq 0$ modes to the ground-state energy of $\mathcal{H} - h\hat{O}$ is the zero-mode energy:

$$E_{\text{GS}} \sim \sum_{k \neq 0} \omega_k = \sum_k \sqrt{(\gamma - f(k) + h)^2 - g^2(k)}. \tag{A.17}$$

Here, the spin-wave dispersion is changed by the addition of the perturbation $-h\sum_i(-1)^i S_i^z$. The second derivative of E_{GS} with respect to h can now be calculated trivially, and in the limit $h \to 0$ we find

$$\chi_{k\neq 0}(\pi) \sim \frac{1}{L}\sum_k \frac{g^2(k)}{\omega_k^3} \tag{A.18}$$

where $g(k)$ was defined before equation (17). As $k \to 0$, $g(k) \to \gamma = \text{const}$, $\omega_k \sim k^{(\alpha-1)/2}$, and therefore

$$\chi_{k\neq 0}(\pi) \sim \frac{1}{L}^{1-3((\alpha-1)/2)} \sim L^{(3\alpha-5)/2}. \tag{A.19}$$

If $\alpha < 3$, this is a smaller power than the L^2 contribution obtained from the $k = 0$ mode. It follows that within the Néel ordered state, the staggered susceptibility scales like L^2 (at least within the spin-wave approximation).

A.3. Transverse correlation function

We now choose

$$\hat{O} = \sum_i S_{i+n}^+ S_i^- \tag{A.20}$$

so that its expectation value $\langle \hat{O} \rangle$ is the transverse contribution to $C(n)$. For simplicity, we assume n to be even (calculations can be done similarly for odd n). Since this is not a Hermitian operator, let

$$\hat{O}_A = \sum_i \left(S_{i+n}^+ S_i^- + S_{i-n}^+ S_i^- \right) \tag{A.21}$$

$$\hat{O}_B = \mathrm{i} \sum_i \left(S_{i+n}^+ S_i^- - S_{i-n}^+ S_i^- \right). \tag{A.22}$$

Both these operators are Hermitian. According to equation (A.1) and using invariance to translations, we then have

$$L\langle S_n^+ S_0^- \rangle = \left\langle \sum_i S_{i+n}^+ S_i^- \right\rangle = \langle \hat{O}_A \rangle - \mathrm{i}\langle \hat{O}_B \rangle \rightarrow \langle S_n^+ S_0^- \rangle = -\frac{1}{L}\left[\frac{\mathrm{d}E_{\mathrm{GS}}^{(A)}}{\mathrm{d}h} - \mathrm{i}\frac{\mathrm{d}E_{\mathrm{GS}}^{(B)}}{\mathrm{d}h} \right] \tag{A.23}$$

where $E_{\mathrm{GS}}^{(A/B)}$ are the ground-state energies in the presence of perturbations $-h\hat{O}_{A/B}$.

A.3.1. The contribution of finite k modes. After a Fourier transform, we use the Holstein–Primakoff representation for all $k \neq 0$ modes. Keeping only quadratic terms, we find

$$\hat{O}_A = 4S \sum_k \cos(nka) \left(b_k^\dagger b_k + a_k^\dagger a_k \right) \tag{A.24}$$

$$\hat{O}_B = 4S \sum_k \sin(nka) \left(b_k^\dagger b_k - a_k^\dagger a_k \right). \tag{A.25}$$

After adding this to the unperturbed Hamiltonian (in the SW approximation) and diagonalizing, we find the ground-state energies to be

$$E_{\mathrm{GS}}^{(A)} = JS \sum_{k\neq0} \omega_{k,A} + 4sh \sum_{k\neq0} \cos(nka) \tag{A.26}$$

$$E_{\mathrm{GS}}^{(B)} = JS \sum_{k\neq0} \omega_{k,B} - 4sh \sum_{k\neq0} \sin(nka) \tag{A.27}$$

where

$$\omega_{k,A} = \sqrt{[\gamma - f(k) - (4h/J)\cos(nka)]^2 - [g(k)]^2} \tag{A.28}$$

$$\omega_{k,B} = \sqrt{[\gamma - f(k) + (4h/J)\sin(nka)]^2 - [g(k)]^2}. \tag{A.29}$$

After taking the first derivatives and setting $h = 0$, we find the $k \neq 0$ modes' contribution to the transverse correlation to be

$$\langle S_n^+ S_0^- \rangle = \frac{2S}{L} \sum_{k \neq 0} \frac{(\gamma - f(k)) \mathrm{e}^{\mathrm{i}kna}}{\omega_k} - \frac{2S}{L} \sum_{k \neq 0} \mathrm{e}^{\mathrm{i}kna}. \tag{A.30}$$

In the limit $k \to 0$, $f(k) \to 0$, $\omega_k \to k^{(\alpha-1)/2}$ and therefore

$$\langle S_n^+ S_0^- \rangle = a_1 L^{(\alpha-3)/2}(1 + \cdots) + 2S/L. \tag{A.31}$$

The second term is the second sum ($\sum_{k \neq 0} \mathrm{e}^{\mathrm{i}kna} = \delta_{n,0}L/2 - 1 = -1$, since $n > 0$). For $\alpha > 2$, the $L^{(\alpha-3)/2}$ term is dominant.

A.3.2. The $k = 0$ mode. Keeping the full $k = 0$ contributions, we find

$$\mathcal{H}_{k=0}(h) = j\vec{S}_1 \cdot \vec{S}_2 - \frac{2h}{L}\left(S_1^+ S_1^- + S_2^+ S_2^-\right). \tag{A.32}$$

The notation was introduced in the previous section. The ground state $|0\rangle$ of $\mathcal{H}_{k=0}$ is known (see the section on staggered susceptibility), so the first order contribution to $E_{\mathrm{GS}}(h)$ can be evaluated directly:

$$L\langle S_n^+ S_0^- \rangle = -\left.\frac{\mathrm{d}E_{\mathrm{GS}}}{\mathrm{d}h}\right|_{h=0} \to \langle S_n^+ S_0^- \rangle = \frac{2}{L^2}\langle 0|S_1^+ S_1^- + S_2^+ S_2^-|0\rangle. \tag{A.33}$$

The calculation is trivial, and we find

$$\langle S_n^+ S_0^- \rangle = \frac{2S^2}{3}\left[1 + \frac{2}{LS}\cdots\right] \sim \frac{1}{L}. \tag{A.34}$$

It follows that for this correlation function the finite k modes give the dominant L dependence, which is $L^{(\alpha-3)/2}$.

This calculation can be repeated for the parallel contribution to the correlation, $\langle S_n^z S_0^z \rangle$. The L dependence remains the same, so we conclude that in the Néel state and within the SW approximation $C(L) \sim L^{(\alpha-3)/2}$.

Appendix B. Large N calculation

Considering the order parameter $\vec{\phi}$ is a N-component unit vector field

$$|\vec{\phi}(\tau, x)|^2 = 1, \tag{B.1}$$

the action can be written as

$$S = \frac{N}{2g}\int \mathrm{d}\tau \, \mathrm{d}x[(\partial\vec{\phi}/\partial\tau)^2 + (\partial\vec{\phi}/\partial x)^2] - \lambda N \int \mathrm{d}\tau \, \mathrm{d}x \, \mathrm{d}y \, \vec{\phi}(\tau, x) \cdot \vec{\phi}(\tau, y)/|x - y|^\alpha. \tag{B.2}$$

We have set $v = 1$. $g \propto 1/s$ is a coupling constant, not related to what we called g in other sections. g and λ are scaled by N in order to have a smooth large N limit. Inside a path integral, we may integrate over all fields $\vec{\phi}(\tau, x)$, without the constraint of equation (B.1), provided that we introduce a Lagrange multiplier field, $\sigma(\tau, x)$:

$$S \to S + \frac{\mathrm{i}N}{2g}\int \mathrm{d}\tau \, \mathrm{d}x \, \sigma(\vec{\phi}^2 - 1). \tag{B.3}$$

The action is now quadratic in unconstrained fields, so that we may, in principle, do the Gaussian integration over $\vec{\phi}$. For this purpose it is convenient to write the long range term in ω–k space using

$$\int_a^\infty \mathrm{d}x \frac{\mathrm{e}^{\mathrm{i}kx}}{|x|^\alpha} \approx \frac{2}{(\alpha-1)} \left(a^{-(\alpha-1)} - |k|^{\alpha-1}\Gamma(2-\alpha)\sin[(2-\alpha)\pi/2] \right). \qquad (\mathrm{B}.4)$$

Here a is a short distance cut-off and this equation is valid for $|k|a \ll 1$. Γ is Euler's Gamma function. Note that the prefactor blows up, $\propto 1/(\alpha-1)$ as $\alpha \to 1$. Note also that for $1 < \alpha < 2$ both $\Gamma(2-\alpha)$ and $\sin[\pi(2-\alpha)/2]$ are >0, so that the second term in equation (B.4) is >0. As $\alpha \to 2$, $\Gamma(2-\alpha) \to 1/(2-\alpha)$ so that $\Gamma(2-\alpha)\sin[\pi(2-\alpha)/2] \to \pi/2$. For $2 < \alpha < 3$, both $\Gamma(2-\alpha)$ and $\sin[\pi(2-\alpha)/2] < 0$ so that their product is positive, blowing up as $\alpha \to 3$.

The first term in equation (B.4) can be eliminated by shifting σ by a (imaginary) constant. Thus we may write

$$S = \frac{NV}{2g} \int \frac{\mathrm{d}\omega\, \mathrm{d}k}{(2\pi)^2} \vec{\phi}(\omega,k)\cdot\vec{\phi}(-\omega,-k)[\omega^2+k^2+C\lambda|k|^{\alpha-1}] + \frac{\mathrm{i}N}{2g}\int \mathrm{d}\tau\, \mathrm{d}x\, \sigma(\vec{\phi}^2-1).$$
$$(\mathrm{B}.5)$$

Here

$$C \equiv \frac{4}{\alpha-1}\Gamma(2-\alpha)\sin[\pi(2-\alpha)/2] \qquad (\mathrm{B}.6)$$

and V is the space–time volume. Now we do the functional integral over $\vec{\phi}$. This gives an effective action for the field σ, which has an overall factor of N in front of it, and no further dependence on N. At large N the functional integral over σ is dominated by a saddle point corresponding to a constant and purely imaginary value of σ. Assuming σ is constant, this effective action is

$$S_{\mathrm{eff}}/V = \frac{N}{2}\left\{ \int \frac{\mathrm{d}\omega\, \mathrm{d}k}{(2\pi)^2} \ln[\omega^2+k^2+C|k|^{\alpha-1}+\mathrm{i}\sigma] - \frac{\mathrm{i}\sigma}{g} \right\}. \qquad (\mathrm{B}.7)$$

The saddle point is found by looking for a stationary point of S_{eff}. Setting $\mathrm{i}\sigma = m^2$ at the saddle point gives the self-consistent equation which determines m^2:

$$\begin{aligned}
\frac{1}{g} &= \int \frac{\mathrm{d}\omega\, \mathrm{d}k}{(2\pi)^2}\frac{1}{\omega^2+k^2+C\lambda|k|^{\alpha-1}+m^2} \\
&= \int_{-\Lambda}^{\Lambda} \frac{\mathrm{d}k}{4\pi}\frac{1}{\sqrt{k^2+C\lambda|k|^{\alpha-1}+m^2}}.
\end{aligned} \qquad (\mathrm{B}.8)$$

Here we have introduced an ultra-violet cut-off, Λ, of $\mathrm{O}(a^{-1})$. For any α, λ and g for which this equation has a solution with $m^2 > 0$, the system is in the disordered phase, with a finite gap, m. Note that, for $\alpha > 3$, the integral diverges as $k \to 0$ when $m = 0$. For small finite m it behaves as $\ln(\Lambda/m)$. Since this diverges as $m \to 0$, there will always be a solution for m, no matter how small is g. On the other hand, for $1 < \alpha < 3$, there

will be a solution for $\lambda < \lambda_c$ only. At the critical value of λ, $m = 0$, so λ_c is determined by

$$\frac{1}{g} = \int_{-\Lambda}^{\Lambda} \frac{\mathrm{d}k}{4\pi} \frac{1}{\sqrt{k^2 + C\lambda_c|k|^{\alpha-1}}}. \tag{B.9}$$

As $\alpha \to 1$, $C \to 4/(\alpha - 1)$ and this becomes

$$\frac{1}{g} = \int_{-\Lambda}^{\Lambda} \frac{\mathrm{d}k}{4\pi} \frac{1}{\sqrt{k^2 + 4\lambda_c/(\alpha - 1)}}. \tag{B.10}$$

Thus we see that $\lambda_c \propto (\alpha - 1)$, as $\alpha \to 1$. $\alpha = 1$ is the critical value of α, for which $\lambda_c \to 0$. The behaviour of $\lambda_c(\alpha)$ is qualitatively similar to what is obtained from SW theory, including the behaviour near $\alpha = 1$. Right at the critical point, the AF spin-correlation function is determined by the effective action with $m = 0$, and $\vec{\phi}$ treated as a non-interacting, free field, in the large N approximation. This implies a dispersion relation

$$\omega = \sqrt{k^2 + C\lambda|k|^{\alpha-1}}, \tag{B.11}$$

and hence a dynamical exponent

$$z = (\alpha - 1)/2. \tag{B.12}$$

This dispersion relation is the same as in SW theory, but there is no long range order at the critical point and hence no ambiguity in the value of z. The spin correlation function is given by

$$\langle \phi^a(\tau, x)\phi^b(0, 0) \rangle = \delta^{ab} \frac{g}{N} \int \frac{\mathrm{d}\omega \, \mathrm{d}k}{(2\pi)^2} \frac{\mathrm{e}^{\mathrm{i}(\omega\tau + kx)}}{\omega^2 + k^2 + C\lambda|k|^{\alpha-1}}. \tag{B.13}$$

In particular, the equal-time correlation function is

$$\langle \phi^a(0, x)\phi^b(0, 0) \rangle = \delta^{ab} \frac{g}{N} \int \frac{\mathrm{d}k}{(4\pi)} \frac{\mathrm{e}^{\mathrm{i}kx}}{\sqrt{k^2 + C\lambda|k|^{\alpha-1}}}. \tag{B.14}$$

At large x, we may approximate this by dropping the k^2 term. It then follows from a rescaling that this decays as

$$\langle \phi^a(0, x)\phi^b(0, 0) \rangle \propto \frac{\delta^{ab}}{|x|^{(3-\alpha)/2}}. \tag{B.15}$$

The standard definition of the critical exponent η then implies

$$z - 1 + \eta = (3 - \alpha)/2, \tag{B.16}$$

giving

$$\eta = 3 - \alpha. \tag{B.17}$$

Note that this is simply the behaviour of the transverse correlation function in the ordered phase, according to SW theory.

To calculate ν, we need to calculate how m vanishes with $\lambda_c - \lambda$ as $\lambda \to \lambda_c$, from below. It turns out that there are two different behaviours, depending on whether $1 < \alpha \leq 5/3$

or $5/3 \leq \alpha < 3$. A small change in λ leads to a change in $1/g$ which is linear in $\delta\lambda$. Consider the effect of a small non-zero m on the gap equation. For $1 < \alpha \leq 5/3$, we may Taylor expand the gap equation:

$$\frac{1}{g} \approx \int_{-\Lambda}^{\Lambda} \frac{\mathrm{d}k}{4\pi} \left[\frac{1}{\sqrt{k^2 + C\lambda|k|^{\alpha-1}}} - (m^2/2)\frac{1}{[k^2 + C\lambda|k|^{\alpha-1}]^{3/2}} \right]. \tag{B.18}$$

(Note that this integral is finite at $k \to 0$ for $(3(\alpha-1)/2 < 1$ only, implying $\alpha < 5/3$.) Setting $\lambda = \lambda_c$, we see that

$$1/g - 1/g_c \propto -m^2. \tag{B.19}$$

Thus $m^2 \propto -\delta\lambda$ in this case. Now consider the equal time correlation function for a small m^2.

$$\langle \phi^a(\tau, x)\phi^b(0, 0) \rangle = \delta^{ab} \frac{g}{N} \int \frac{\mathrm{d}k}{(4\pi)} \frac{\mathrm{e}^{\mathrm{i}kx}}{\sqrt{k^2 + C\lambda|k|^{\alpha-1} + m^2}}. \tag{B.20}$$

At large distances and small m^2 we should be able to drop the k^2 term and ignore the ultra-violet cut-off. A rescaling of the k-integration variable then implies a correlation length

$$\xi \propto m^{-2/(\alpha-1)} \propto (\delta\lambda)^{-1/(\alpha-1)} \tag{B.21}$$

and hence an exponent

$$\nu = 1/(\alpha - 1), \qquad (1 < \alpha \leq 5/3). \tag{B.22}$$

Now consider the case $5/3 \leq \alpha < 3$. Keeping a small non-zero m^2, we find

$$\frac{\mathrm{d}}{\mathrm{d}m^2}\left(\frac{1}{g}\right) = \frac{-1}{2} \int \frac{\mathrm{d}k}{4\pi} \frac{1}{[\lambda C|k|^{\alpha-1} + m^2]^{3/2}}. \tag{B.23}$$

Since the integral is dominated by $|k|$ of $\mathrm{O}(m^{2/(\alpha-1)})$, we have taken the cut-off to infinity and dropped the k^2 term. By scaling, we see that

$$\frac{\mathrm{d}}{\mathrm{d}m^2}\left(\frac{1}{g}\right) \propto m^{(5-3\alpha)/(\alpha-1)}. \tag{B.24}$$

Integrating with respect to m^2 gives

$$\frac{1}{g} \approx \frac{1}{g_c} - Am^{(3-\alpha)/(\alpha-1)}, \tag{B.25}$$

for a constant, A. Thus we see that

$$m \propto (-\delta\lambda)^{(\alpha-1)/(3-\alpha)}. \tag{B.26}$$

This gives

$$\xi \propto m^{-2/(\alpha-1)} \propto (-\delta\lambda)^{-2/(3-\alpha)}. \tag{B.27}$$

Thus

$$\nu = \frac{2}{3 - \alpha}, \qquad (5/3 \leq \alpha < 3). \tag{B.28}$$

References

[1] Affleck I, Gelfand M P and Singh R R P, 1994 *J. Phys. A: Math. Gen.* **27** 7313
[2] Haldane F D M, 1983 *Phys. Rev. Lett.* **50** 1153
    Affleck I and Haldane F D M, 1987 *Phys. Rev.* B **36** 5291
[3] Affleck I, Gepner D, Schulz H J and Ziman T, 1989 *J. Phys. A: Math. Gen.* **22** 511
    Giamarchi T and Schulz H J, 1989 *Phys. Rev.* B **39** 4620
[4] Haldane F D M, 1988 *Phys. Rev. Lett.* **60** 635
    Shastry S, 1988 *Phys. Rev. Lett.* **60** 639
[5] Mermin N D and Wagner H, 1966 *Phys. Rev. Lett.* **17** 1133
[6] Ruelle D, 1968 *Commun. Math. Phys.* **9** 267
    Dyson F J, 1969 *Commun. Math. Phys.* **12** 212
    Thouless D J, 1969 *Phys. Rev.* **187** 732
[7] Fisher M E, Ma S-K and Nickel B G, 1972 *Phys. Rev. Lett.* **29** 917
[8] Kosterlitz J M, 1976 *Phys. Rev. Lett.* **37** 1577
[9] Brezin E, Zinn-Justin J and Le Guillou J-C, 1976 *J. Phys. A: Math. Gen.* **9** L119
[10] Cardy J L, 1981 *J. Phys. A: Math. Gen.* **14** 1407
[11] Fröhlich J and Spencer T, 1982 *Commun. Math. Phys.* **84** 87
[12] Luijten E and Messingfeld H, 2001 *Phys. Rev. Lett.* **86** 5305
[13] Bruno P, 2001 *Phys. Rev. Lett.* **87** 137203
[14] Yusuf E, Joshi A and Yang K, 2004 *Phys. Rev.* B **69** 144412
[15] Parreira J R, Bolina O and Perez J F, 1997 *J. Phys. A: Math. Gen.* **30** 1095
[16] Syljuasen O F and Sandvik A W, 2002 *Phys. Rev.* E **66** 046701
[17] Sandvik A W, 2003 *Phys. Rev.* E **68** 056701
[18] Cardy J, 1996 *Scaling and Renormalization in Statistical Physics* (Cambridge: Cambridge University Press) chapter 4
[19] Blöte H W J, Cardy J L and Nightingale M P, 1986 *Phys. Rev. Lett.* **56** 742
    Affleck I, 1986 *Phys. Rev. Lett.* **56** 746
[20] Holstein T and Primakoff H, 1940 *Phys. Rev.* **58** 1098
[21] Reger J D and Young A P, 1988 *Phys. Rev.* B **37** 5978
[22] Ma S-K, 1973 *Phys. Rev.* A **7** 2172
[23] Sak J, 1977 *Phys. Rev.* B **15** 4344
[24] Bhattacharjee J, Cardy J L and Scalapino D J, 1982 *Phys. Rev.* B **25** 1681